DIRECTING CELLULAR TRAFFIC USING GEOMETRIC AND BIOMOLECULAR CUES

Thesis by

Keiichiro Kushiro

In partial fulfillment of the requirements

for the degree of

Doctor of Philosophy

CALIFORNIA INSTITUTE OF TECHNOLOGY

Pasadena, California

2011

(Defended September 22, 2010)

ACKNOWLEDGEMENTS

Above all, I would like to thank my research advisor, Prof. Anand Asthagiri, for his continued support and guidance throughout my graduate studies. His boundless knowledge, sharp insights and pursuit for excellence have contributed tremendously in the making of the exciting projects discussed in this thesis. It was a pleasure to be able to work with him on the forefront of science and to be given the opportunity to push the envelope in a new field of research.

I would also like to thank other great faculty and staff, whose support were invaluable in making my life at Caltech professionally rewarding. I would like to start by thanking my thesis committee members, Prof. David Tirrell, Prof. Paul Sternberg and Prof. Marianne Bronner-Fraser, for their friendliness, encouragement and useful advice. I would also like to thank Prof. Chin-lin Guo for his friendship and expertise. In addition, I would like to thank Guy DeRose, Alireza Ghaffari, Christina Morales and Saurabh Vyawahare for facilitating my experience at Kavli Nanoscience Institute (KNI) at Caltech. Lastly, I would like to show my appreciation to the wonderful ladies, Kathy Bubash, Laura King, Martha Hepworth and Alison Ross, for taking care of various administrative issues and fixing problems in the lab.

Next, I would like to thank the past (Claudiu Giurumescu, Nicholas Graham, Niki Galownia, Stephen Chapman and Ehsan Jabbarzadeh) and current (Jin-Hong Kim, Melissa Pope, Larry Dooling and Paul Minor) lab members from the Asthagiri lab who made the lab intellectually and socially enjoyable. On top of all the science I learned from you, I

enjoyed the various lunch discussions spanning international politics, religious beliefs, baby care and my non-Japanese behaviors. I would also like to thank my wonderful undergraduates, Stephanie Chang and Amy Proctor, who worked hard and made great progress during the summer. I wish all of you great success in your academic careers and hope for more interactions in years to come.

Life at Pasadena would have been little short of disastrous if it were not for all the help and company provided by my good friends. In particular, I would like to thank my colleague Jin-Hong Kim and long time roommate Mike Chen for all the fun we had together like the 'traumatic trip' to Japan, 'total loss' at Las Vegas, 'total win' online and 'Barbie Girl / Spiderman' karaoke parties, as well as countless rides and celebrations I received. Although I cannot mention everyone that I am thankful for, including friends from other labs, institutions and countries, I do want them to know that I would not have survived Pasadena without their friendship to maintain sanity and order in my life.

Finally, I cannot thank my family (Dad, Mom, Kyoko and Taishi) enough for their unconditional love and support. Despite being a few countries away, your presence has always been felt inside of me during my tortuous journey to complete this thesis. You made me who I am today, and I am very proud of and grateful for who I have become. Thank you, and thank you all ever so much.

ABSTRACT

Directing Cellular Traffic Using Geometric and Biomolecular Cues

September 2010

Directed cell migration plays a principal role in various aspects of important cellular phenomena such as wound healing, development and cancer metastasis. Although the mechanism of gradient stimulus leading to directed cell migration is well understood and exploited, the geometrical and topographical cues that cause directed migration has been largely unexplored. With the advent of accessible microfabrication techniques to precisely control the topography of the extracellular matrix (ECM) on substrates, researchers are just starting to study the complex mechanical signals that can alter directed cell motility. A key challenge now is to parse out the precise factors that affect directional movement of cells on certain micropatterns, use that understanding to design strategies to enhance the motility and bias of directed cell migration, and further apply these concepts to multiple cell types and higher-order cell systems.

Here, we investigate the tunability of directional bias through various geometrical manipulations using quantitative analysis of cell movement on micropatterns. We observe that MCF-10A epithelial cells in general jump with an unnaturally high bias between teardrop-based islands with specific gap distance, asymmetry and positional placement. Throughout the studies, we observe that lamellipodial protrusions and unilamellar

morphology play a crucial role in dictating not only the directional bias of epithelial cells, but also their speed and persistence, and find that moderate alteration of Rac1 signal leads to an unexpected flip of bias. We further extend the concept of directional bias to design patterns to successfully control cell flux and effectively partition cell population, as well as induce unilamellar morphology in different cell types to promote directed cell motility. We also investigate the combinatorial effect of hybrid micropatterns in enhancing motility and unravel the unique properties and possible mechanisms behind directed cell motility on teardrop-based micropatterns.

Our results demonstrate a new type of directed cell motility using a micropattern that involves the use of physical constraints to stabilize the unilamellar morphology and guidance of the unilamella in the correct direction through purely geometrical cues. These studies offer multiple design strategies to modulate the cell motility and directional bias on micropatterns for various applications, such as tissue engineering.

TABLE OF CONTENTS

Acknowledgements iii

Abstract v

Table of Contents vii

List of Tables xii

List of Figures xiii

Chapter I: Overview I-1

1. Introduction I-1
2. Directed cell migration I-2
    - 2.1. Mechanism and regulation of polarized cell motility I-2
    - 2.2. Key signaling molecules associated with polarized migration I-3
3. Microfabricated systems to control cell motility I-4
4. Unresolved questions on directed cell motility on micropatterns I-6
5. Current results I-8
6. References I-10

Chapter II: Reprogramming Directional Cell Motility by Tuning Micropattern Features and Cellular Signals II-1

1. Abstract II-1

2. Introduction II-2

3. Results II-2

3.1. Key pattern features are necessary for directional cell motility II-2

3.2. Geometrical modification based on quantitative jump analysis enhances directional bias II-4

3.3. Signal alteration based on lamellipodial observations flips directional bias II-6

3.4. Novel splitter design modulates cell flux II-9

4. Conclusion II-10

5. Experimental Methods II-11

5.1. Fabrication of micropatterned substrates II-11

5.2. Cell culture II-12

5.3. Time-lapse microscopy II-12

5.4. siRNA knockdown II-13

6. Acknowledgements II-13

7. References II-13

8. Supporting Information II-15

8.1. Supporting figures II-15

8.2. Supporting table II-18

8.3. Movie legends II-18

Chapter III: A Hybrid Micropattern Design for Supraoriented Cell Movement and Enhanced Multicellular Partitioning III-1

1. Abstract III-1
2. Introduction III-2
3. Results III-3
    - 3.1. Line patterns markedly enhance persistence in addition to cell speed III-3
    - 3.2. A hybrid micropattern design that combines line and teardrop features III-4
    - 3.3. The hybrid spear-shaped micropattern markedly improves the directional bias of cell movement III-7
    - 3.4. Hybridizing line and teardrop micropatterns yields an additive improvement in the persistence of cell migration III-8
    - 3.5. Reduced frequency of hops lead to improvements in migration speed on spear-shaped micropatterns III-10
    - 3.6. Micropatterned bridges with hybrid patterns result in a rapid and effective partitioning across long distances III-12
4. Conclusion III-16
5. Experimental Methods III-17

5.1. Fabrication of micropatterned substrates III-17

5.2. Cell culture III-18

5.3. Time-lapse microscopy.....III-18

5.4. Data collection and analysis III-19

6. Acknowledgements III-20

7. References III-20

Chapter IV: Scaling Micropattern Dimensions to Enable and Modulate Directed Cell Movement IV-1

1. Abstract..... IV-1

2. Introduction IV-2

3. Results IV-3

3.1. Cell types differ in the extent of directional bias on teardrop patterns IV-3

3.2. Establishment of unilamellar morphology correlates with extent of directed cell movement on teardrop patterns IV-6

3.3. Narrowing teardrop patterns enhances directional bias..... IV-8

4. Future Directions..... IV-11

5. Conclusion..... IV-12

6. Experimental Methods IV-13

6.1. Fabrication of micropatterned substrates IV-13

6.2. Cell culture IV-14

6.3. Time-lapse microscopy IV-15

6.4. Cell motility quantitation and analysis IV-16

7. Acknowledgements IV-16

8. References IV-16

9. Supplementary Data IV-16

LIST OF TABLES

Chapter II

Table S1. Detailed analysis of the jumps of MCF-10A epithelial cells from either blunt or tip ends over two experiments II-18

Chapter III

Table 1. Enhanced motility of MCF-10A epithelial cells on line patterns ... III-4

Table 2. Detailed analysis of hop decisions at corners and residence times associated with the events III-8

Table 3. Cell motility on teardrop patterns and spear-shaped patterns III-9

Chapter IV

Table 1. Tendency to acquire FR polarity for MCF-10A epithelial cells, NHEKs and Rat1 fibroblasts on line patterns of different widths..... IV-8

LIST OF FIGURES

Chapter II

Figure 1. Directional bias of MCF-10A epithelial cells on teardrop-based micropatterns II-5

Figure 2. The role of lamellipodial extensions in determining the directional bias of cell movement on micropatterns II-8

Figure 3. The effect of splitter design features on the directional bias II-10

Figure S1. Directional bias of normal human epidermal keratinocytes (NHEK) on Patterns A and B II-15

Figure S2. Morphology of migrating MCF-10A epithelial cells and Rat1 fibroblasts II-16

Figure S3. Effect of RNA interference on Rac1 expression level..... II-17

Figure S4. Fluorescence imaging of the underlying micropattern via BSA-Cy3 ..... II-17

Chapter III

Figure 1. Schematic and directional bias of teardrop and spear-shaped patterns..... III-6

Figure 2. Schematic and effectiveness of partition patterns with Spear-shaped and teardrop bridges III-12

Chapter IV

Figure 1. Motility biases for MCF-10A epithelial cells, NHEKs and Rat1 fibroblasts on the original teardrop patterns IV-5

Figure 2. Motility biases for MCF-10A epithelial cells and NHEKs on thin teardrop patterns..... IV-10

Figure 3. Schematics of thin rectangles and extra thin teardrop patterns to be tested with MCF-10A cells, NHEKs and other cell lines IV-12

Chapter I: Overview

1. Introduction

Cell motility governs many aspects of life including embryogenesis, immune response and wound healing. Basic mechanisms of random cell migration are well understood and many signaling pathways associated with motility have been unraveled.[1, 2] However, much like how random movement of molecules does not yield complex activities within a living cell, random motility does not result in the intricate, multicellular processes that govern many biological phenomena.

More specifically, directional migration of cells is a crucial component of cell motility that involves multifaceted regulation, whose precise orchestration is vital for biological development and various responses in the body. For example, neural crest cells must migrate in a highly persistent and ordered fashion during embryogenesis and failure of these cells to do so can result in life threatening, developmental consequences.[3] Furthermore, directed migration plays an important role in pathologies such as chronic inflammatory diseases and tumor metastasis, and inhibitors of directed migration provide a promising venue for treatment.[4, 5]

In directional migration, multiple factors operate at various steps of cell migration to control the stability and direction of lamellipodia. Such factors include topography of the extracellular matrix (ECM),[6-8] receptor signaling and adhesion molecule trafficking,[9, 10] myosin contraction[11, 12] and cell polarity machinery.[5, 13] Many of these

cues converge at the Rho-family GTPases, such as the Rac1 and Cdc42 molecules, to regulate the lamellipodial protrusions that ultimately dictate the bias of directional cell migration.

Although multitudes of gradient-based systems have been used to induce directional cell migration,[14-16] there are many innate limitations that cannot be overcome. Recently, researchers have begun to look into the possibility of a more robust and stable form of directional control using micropatterns that does not require any stimulus gradient or external field. Micropatterning techniques offer precise control over the topography of the ECM and allow for more sophisticated design strategies to enhance, modulate and govern directional cell migration.

2. Directed cell migration

2.1. Mechanism and regulation of polarized cell motility

Net cellular movement in one direction is caused by the asymmetric morphology of a migrating cell with defined leading and trailing edges. Cell motility in the direction of the leading edge is orchestrated by the classic cell motility cycle: polarized intracellular signaling orients protrusions at the lamellipodium of the leading edge, integrins form new adhesions to the substrate in the lamellipodium, and myosin contraction leads to preferential detachment of adhesions in the trailing edge.[1, 2, 17] In many cases, direction of migration is determined by the orientation of the most stable protrusion, and thus cells maintain directionally persistent migration by regulating the

number and orientation of lamellipodia through internal signaling and external cues.[18, 19] Also, new lamellipodial protrusions are often locally generated from pre-existing leading edge instead of randomly across the periphery of a cell and extend laterally from the main longitudinal axis of the cell,[20, 21] and as a result there is usually a gradual sideways shift of lamellipodium when cells do change direction (i.e., cells rarely change direction 180° without external regulation).

Directional cell migration can be caused by intrinsic cell directionality or through various external regulations. Cells with high intrinsic directionality, such as fish epidermal keratocytes, travel less randomly and migrate with high persistence.[22] However, in order to control multiple cells to migrate in the same direction, external regulation must be applied. Such external cues are often gradient-based and include: soluble molecules (chemotaxis),[14, 23] adhesivity to the underlying substrate (haptotaxis),[15, 24] rigidity (durotaxis)[16, 25] and electric field (electrotaxis).[26] However, these gradient-based methods have certain limitations, such as the necessity of the gradient (as a result, cells can only travel a certain distance often in a linear path at a rate proportional to the steepness of the gradient) and inability to control cells individually.

2.2. Key signaling molecules associated with polarized migration

Although the entirety of signaling networks associated with directed migration is complex and still not fully understood, the roles of certain key molecules, namely Par complexes and Rho-family of GTPases, in establishing cell polarity and directed migration are starting to be clear.[13, 27] The Par (partitioning defective) complex

molecules, such as Par3, Par6 and aPKC, are part of the cellular polarity signaling machinery that establish the front-rear (FR) polarity of the cells.[5] Rho-family of GTPases, such as Cdc42, Rac1 and RhoA, are small GTPases that regulate the actin dynamics within the cell.[28] The complex crosstalk among these polarity proteins and small GTPases, as well as other molecules like integrins, Wnt5a and Syndecan 4, largely regulate cell polarization in different cellular contexts across different cell types.[10, 11, 29-33]

In particular, the small GTPase Rac1, which regulates the local actin polymerization at the lamellipodia, has been recently identified as a central determinant for random versus directional motility. High level of Rac1 activity results in the formation of multiple lamellae and lead to non-directional cell movement, while moderate level of Rac1 result in fewer lateral lamellae and lead to directional migration.[34, 35] In addition, mutual inhibition of Rac1-mediated protrusion at the leading edge and RhoA-mediated myosin contraction at the trailing edge has been implicated to aid the stability of FR polarity.[11, 12]

3. Microfabricated systems to control cell motility

Although the concept of contact guidance, the process by which cells are guided by topographical structures, was introduced decades ago,[6, 7, 36] precise physical and geometrical cues for guiding the organization and migration of cells were largely unexplored until recently. Now, the readily available microfabrication techniques have enabled researchers to create well-defined geometrical systems to study how the cells

probe their physical surroundings and acquire mechanical information or signals. Over the past decade, researchers have successfully used microfabrication techniques to control various cell behaviors such as cell shape, survival, differentiation and cell-cell contact.[37-41] However, there has been only limited work on the use of micropatterns to influence cell motility, and thus far, only two main types of micropatterns aimed to geometrically control cell motility exist: line patterns (steps and grooves) and asymmetric patterns (teardrop-shaped).

Line patterns are arrays of straight adhesive tracks; steps and grooves are similar in concept but have an added 3D topography of side walls. Line patterns (steps and grooves) are generally used to polarize and physically limit the movement of cells to one axis and are even effective at nanometer length scales,[36, 42-44] though the direction of movement on the line remains bidirectional (i.e., cells can travel up or down a line). Similarly, arrays of rectangular islands that approximate focal adhesion sizes can be used to control the axis of cell migration, but not the direction of migration.[45] Nonetheless, line patterns at length scales of single cells or below are becoming useful, high-throughput *in vitro* model systems to replicate and study migratory behaviors of cells in natural systems, such as 3D migration through fibrillar matrix[46] and tumor metastasis through blood vessels.[47]

Asymmetric (teardrop-shaped) micropatterns are designed to control the direction of cell movement and are often based on teardrop-shaped islands with a broad, rounded end (‘blunt’ end) and narrow, thin edge (‘tip’ end). Whitesides and colleagues first used such asymmetric geometry to confine and subsequently direct the cell movement after

release from confinement,[48] but this spontaneous bias disappeared shortly after the release of the cells. Recently, Grzybowski and colleagues used a series of asymmetric ratchets to guide cell populations, but due to the very low innate directional bias of the pattern, partitioning and sorting was only partially achieved.[49] All in all, there has been only one successful demonstration of effective and prolonged directed cell motility using micropatterns, and it was by Co and colleagues who utilized four teardrop-shaped adhesive islands set up in a square configuration to induce unidirectional movement of fibroblasts around the islands.[50] These studies suggest that physical interactions of the cells with underlying topography of ECM, independent of chemical factors, can induce responses and signaling to promote directional migration.

4. Unresolved questions on directed cell motility on micropatterns

Because of the limited number and extent of studies with successful directed cell motility using micropatterns, there are many unresolved questions to be addressed. The first and most relevant question is on the mechanism of directed motility on micropatterns, or in other words, why and how do the cells move in a biased fashion? Co and others suggest that the elongated polarization of the cells on the island and the availability of the adjacent islands along the polarized axis cause the directional bias.[50] However, they do not sufficiently address why the cells move to the adjacent island once the lamellipodial extension is made (i.e., why there is a net translocation to the next island). Furthermore, they specify polarization as an important factor for directional bias, but do not explore or alter the degree of polarization in their work. Thus, we still do not

completely understand the cause of directional bias, nor the precise factors contributing to directed cell motility on micropatterns.

The second question is on the generality and robustness of the directed cell motility observed thus far. Co and others have tested their patterns on 3T3 fibroblasts and human microvascular endothelial cells (HMVECs) and confirmed directed movement.[50] However, would other cell lines interpret the underlying geometry differently? In addition, would the bias be in the same direction as previously observed and would the mechanism of directed motility be the same? Although different cell lines are expected to exhibit different motility tendencies and have been observed to do so,[51, 52] it may be worthwhile to explore commonalities between cell types that exhibit similar directional bias and behavior to elucidate the key factors that govern directed cell motility. For example, could it be a specific signaling pathway involved or the morphology they assume under mechanical constraint?

The third question is on strategies to optimize and modulate directed motility, as well as future directions and applications. We have thus far only observed the phenomenon of directed motility through micropatterns, but have not seen any attempt to modulate it through experimental manipulations. Can the directional bias be enhanced or controlled through geometrical alteration of the underlying micropatterns or re-wiring of cell signals and mechanics? Furthermore, as we begin to understand the mechanism of directed cell motility on micropatterns and be able to control it, how can we utilize it for greater applications?

This report aims to answer some of these questions and shed light on this largely unexplored field of directed cell motility using micropatterns.

5. Current results

In this report, we investigate the phenomena of directed cell motility on micropatterns from different angles, explore various factors that affect this phenomena and design strategies based on our observations and hypotheses to enhance or change the directional bias. We also address the concept of single cell versus multicellular manipulation and responses of different cell types on these micropatterns. Overall, the chapters in this report build up in a logical order and may be best followed in sequential order.

Chapter II focuses on the basic single cell analysis of directional bias of cells on teardrop-based micropatterns. Starting from micropatterns proven to be effective in previous studies,[50] we elucidate the fundamental pattern parameters crucial for the directed movement of MCF-10A epithelial cells. Through quantitative analysis of cell motility, we identify highly favored hops and design new patterns to enhance the directional bias. We also closely examine the favored hops and notice the involvement of sideways lamellipodial protrusion. Based on this observation, we hypothesize that altering the Rac1 signal pathway involved in lamellipodial protrusion may change the directional bias and demonstrate that indeed that is the case. In addition, we introduce the splitter motif designed to modulate the flux of cells.

Chapter III focuses on the motility of cells, such as speed and persistence length, and how different motifs of micropatterns can be combined to create a novel, hybrid pattern with enhanced motility. Here, we examine the motility and persistence of MCF-10A cells on line patterns, and find that specific line width optimally enhances the speed and persistence of cells. We proceeded to combine the enhanced motility of line patterns and the directional bias of teardrop-based patterns to create a hybrid pattern, which excels both the original patterns in terms of motility. Through quantitative comparison of cell movement on the classic teardrop pattern and the hybrid pattern, we found that the line component in the hybrid pattern allows the cells to travel longer distances without having to pause at junctions and thus result in enhanced speed and persistence. This chapter also introduces higher-order partition patterns to direct the motility of cell populations. Studies with multicellular systems reveal complexities that were not observed in single cell systems. Nonetheless, the effectiveness of the partition patterns surpass any previously reported pattern-based partitioning.[49]

Chapter IV focuses on the establishment of front-rear (FR) polarity and scaling of micropatterns to enable directed motility for different cell lines. Here, we examine the directional bias of various cell types on the classic teardrop patterns and find that cells with high bias assume a unilamellar morphology with heavily one-sided FR polarity, while the cells with no bias fail to do so. Based on previous studies,[46] we investigate the relationship between the establishment of unilamellar morphology and the physical constraint imposed by the line micropattern, and find that the fraction of cells with unilamellar morphology correlates with the degree of physical constraint (i.e., line width). Thus, in order to increase the directional bias for moderately biased cell line, we design

thin teardrop patterns with decreased width. Indeed, the directional bias increases significantly for the previously moderately biased cell line, but more surprisingly, certain configurations which were not biased with the original teardrop now become biased with the thin teardrop. This suggests that the degree of physical constraint is not only important for the establishment of FR polarity, but is also a crucial factor for dictating the directional tendencies at the ends of the teardrop islands.

Together, these studies deepen our understanding on directed cell motility using micropatterns, offer several strategies to enhance the motility and directional bias for different cell lines, and lay a foundation for wider application using micropatterns such as cell sorting and tissue engineering.

6. References

[1] D. A. Lauffenburger, A. F. Horwitz, *Cell* **1996**, *84*, 359.

[2] A. J. Ridley, M. A. Schwartz, K. Burridge, R. A. Firtel, M. H. Ginsberg, G. Borisy, J. T. Parsons, A. R. Horwitz, *Science* **2003**, *302*, 1704.

[3] J. M. Teddy, P. M. Kulesa, *Development* **2004**, *131*, 6141.

[4] C. R. Mackay, *Nat Immunol* **2008**, *9*, 988.

[5] S. Etienne-Manneville, *Oncogene* **2008**, *27*, 6970.

[6] P. Weiss, B. Garber, *Proc Natl Acad Sci U S A* **1952**, *38*, 264.

[7] B. Garber, *Exp Cell Res* **1953**, *5*, 132.

[8] M. Sidani, J. Wyckoff, C. Xue, J. E. Segall, J. Condeelis, *J Mammary Gland Biol Neoplasia* **2006**, *11*, 151.

[9] P. T. Caswell, J. C. Norman, *Traffic* **2006**, *7*, 14.

[10] T. Nishimura, K. Kaibuchi, *Dev Cell* **2007**, *13*, 15.

[11] K. N. Pestonjamasp, C. Forster, C. Sun, E. M. Gardiner, B. Bohl, O. Weiner, G. M. Bokoch, M. Glogauer, *Blood* **2006**, *108*, 2814.

[12] A. Van Keymeulen, K. Wong, Z. A. Knight, C. Govaerts, K. M. Hahn, K. M. Shokat, H. R. Bourne, *J Cell Biol* **2006**, *174*, 437.

[13] S. Iden, J. G. Collard, *Nat Rev Mol Cell Biol* **2008**, *9*, 846.

[14] H. R. Bourne, O. Weiner, *Nature* **2002**, *419*, 21.

[15] J. B. McCarthy, S. L. Palm, L. T. Furcht, *J Cell Biol* **1983**, *97*, 772.

[16] J. Y. Wong, A. Velasco, P. Rajagopalan, Q. Pham, *Langmuir* **2003**, *19*, 1908.

[17] M. P. Sheetz, D. Felsenfeld, C. G. Galbraith, D. Choquet, *Biochem Soc Symp* **1999**, *65*, 233.

[18] F. J. Martini, M. Valiente, G. Lopez Bendito, G. Szabo, F. Moya, M. Valdeolmillos, O. Marin, *Development* **2009**, *136*, 41.

[19] R. S. Fischer, M. Gardel, X. Ma, R. S. Adelstein, C. M. Waterman, *Curr Biol* **2009**, *19*, 260.

[20] C. Arrieumerlou, T. Meyer, *Dev Cell* **2005**, *8*, 215.

[21] N. Andrew, R. H. Insall, *Nat Cell Biol* **2007**, *9*, 193.

[22] J. Lee, A. Ishihara, J. A. Theriot, K. Jacobson, *Nature* **1993**, *362*, 167.

[23] S. H. Zigmond, *J Cell Biol* **1977**, *75*, 606.

[24] S. B. Carter, *Nature* **1965**, *208*, 1183.

[25] C. M. Lo, H. B. Wang, M. Dembo, Y. L. Wang, *Biophys J* **2000**, *79*, 144.

[26] M. Zhao, *Semin Cell Dev Biol* **2009**, *20*, 674.

[27] R. J. Petrie, A. D. Doyle, K. M. Yamada, *Nat Rev Mol Cell Biol* **2009**, *10*, 538.

[28] A. B. Jaffe, A. Hall, *Annu Rev Cell Dev Biol* **2005**, *21*, 247.

[29] E. E. Sander, J. P. ten Klooster, S. van Delft, R. A. van der Kammen, J. G. Collard, *J Cell Biol* **1999**, *147*, 1009.

[30] O. Pertz, L. Hodgson, R. L. Klemke, K. M. Hahn, *Nature* **2006**, *440*, 1069.

[31] M. Nakayama, T. M. Goto, M. Sugimoto, T. Nishimura, T. Shinagawa, S. Ohno, M. Amano, K. Kaibuchi, *Dev Cell* **2008**, *14*, 205.

[32] K. Schlessinger, E. J. McManus, A. Hall, *J Cell Biol* **2007**, *178*, 355.

[33] M. D. Bass, K. A. Roach, M. R. Morgan, Z. Mostafavi-Pour, T. Schoen, T. Muramatsu, U. Mayer, C. Ballestrem, J. P. Spatz, M. J. Humphries, *J Cell Biol* **2007**, *177*, 527.

[34] R. Pankov, Y. Endo, S. Even-Ram, M. Araki, K. Clark, E. Cukierman, K. Matsumoto, K. M. Yamada, *Journal of Cell Biology* **2005**, *170*, 793.

[35] L. Vidali, F. Chen, G. Cicchetti, Y. Ohta, D. J. Kwiatkowski, *Mol Biol Cell* **2006**, *17*, 2377.

[36] A. Wood, *J Cell Sci* **1988**, *90 (Pt 4)*, 667.

[37] R. Singhvi, A. Kumar, G. P. Lopez, G. N. Stephanopoulos, D. I. C. Wang, G. M. Whitesides, D. E. Ingber, *Science* **1994**, *264*, 696.

[38] R. McBeath, D. M. Pirone, C. M. Nelson, K. Bhadriraju, C. S. Chen, *Developmental Cell* **2004**, *6*, 483.

[39] C. S. Chen, M. Mrksich, S. Huang, G. M. Whitesides, D. E. Ingber, *Science* **1997**, *276*, 1425.

[40] M. Thery, V. Racine, M. Piel, A. Pepin, A. Dimitrov, Y. Chen, J. B. Sibarita, M. Bornens, *Proc Natl Acad Sci U S A* **2006**, *103*, 19771.

[41] C. M. Nelson, C. S. Chen, *J Cell Sci* **2003**, *116*, 3571.

[42] D. M. Brunette, *Exp Cell Res* **1986**, *167*, 203.

[43] P. Clark, P. Connolly, A. S. Curtis, J. A. Dow, C. D. Wilkinson, *J Cell Sci* **1991**, *99 (Pt 1)*, 73.

[44] W. A. Loesberg, J. te Riet, F. C. van Delft, P. Schon, C. G. Figdor, S. Speller, J. J. van Loon, X. F. Walboomers, J. A. Jansen, *Biomaterials* **2007**, *28*, 3944.

[45] N. Xia, C. K. Thodeti, T. P. Hunt, Q. Xu, M. Ho, G. M. Whitesides, R. Westervelt, D. E. Ingber, *FASEB J* **2008**, *22*, 1649.

[46] A. D. Doyle, F. W. Wang, K. Matsumoto, K. M. Yamada, *J Cell Biol* **2009**, *184*, 481.

[47] D. Irimia, M. Toner, *Integr Biol (Camb)* **2009**, *1*, 506.

[48] X. Jiang, D. A. Bruzewicz, A. P. Wong, M. Piel, G. M. Whitesides, *Proc Natl Acad Sci U S A* **2005**, *102*, 975.

[49] G. Mahmud, C. J. Campbell, K. J. M. Bishop, Y. A. Komarova, O. Chaga, S. Soh, S. Huda, K. Kandere-Grzybowska, B. A. Grzybowski, *Nature Physics* **2009**, *5*, 606.

[50] G. Kumar, C. C. Ho, C. C. Co, *Advanced Materials* **2007**, *19*, 1084.

[51] S. Huang, C. P. Brangwynne, K. K. Parker, D. E. Ingber, *Cell Motil Cytoskeleton* **2005**, *61*, 201.

[52] K. Wolf, I. Mazo, H. Leung, K. Engelke, U. H. von Andrian, E. I. Deryugina, A. Y. Strongin, E. B. Brocker, P. Friedl, *Journal of Cell Biology* **2003**, *160*, 267.

Chapter II: Reprogramming Directional Cell Motility by Tuning Micropattern Features and Cellular Signals

1. Abstract

Mammalian cells exhibit directed cell movement on micropatterned surfaces.[1-3] A key challenge is to better understand the parameters and mechanisms that orient cell movement on micropatterns and to apply these insights to modulate rationally cellular traffic on synthetic materials. Here, using quantitative insights gleaned from the analysis of cell movement on teardrop-shaped micropatterns, we re-design the geometrical features of micropatterns to enhance the directional bias and to modulate the flux of cell movement. Furthermore, we demonstrate that perturbing an intracellular signal involved in lamellipodial extensions (Rac1) flips the preferred direction of cell movement. Our findings reveal a key role for lamellipodial extensions in determining the directional bias of cell movement on micropatterns and offer design strategies to modulate and reprogram this bias by manipulating pattern features and cellular signals. These insights begin to lay a foundation for constructing materials for channeling cellular traffic in applications, such as tissue engineering.

Reprinted from K. Kushiro and A.R. Asthagiri from *Advanced Materials* (2010).

2. Introduction

Micropatterned surfaces have been used effectively to control cell shape, survival, proliferation and differentiation.[4-6] More recently, it has been shown that cells can exhibit persistent, directional movement on micropatterned surfaces.[2,3] When cells were released from confinement within a teardrop-shaped micropattern, their initial trajectory favored the blunt end over the tip end.[1] This short-lived bias is consistent with the stereotypical teardrop-like shape ascribed to a migrating cell with a broad leading edge and a narrow trailing tail.[7,8] A more persistent bias in cell movement was observed on a micropattern composed of four disjointed teardrop-shaped islands that are arranged to form a square.[2] On this pattern, the asymmetry of the teardrop defined a major axis for the cell body, but the direction of movement did not favor the blunt or tip end. The direction was dictated by the availability of an adjacent island along the cell body axis.

3. Results

3.1. Key pattern features are necessary for directional cell motility

In this work, we sought to better understand the micropattern features and cellular signals that orient cell movement on micropatterns and to apply these insights to rationally modulate and re-program the directional bias of cell movement. To begin our study, we used the teardrop-shaped micropatterns described previously[2] and quantified the movement tendencies of MCF-10A mammary epithelial cells. The percentage of complete jumps that were made in either direction of the pattern was measured (**Fig. 1**, labeled arrows). Teardrop islands in Pattern A (**Fig. 1A** and **Movie 1**) induced a strong

directional bias in which 81% of the jumps were observed to be sideways from the tip of a teardrop to the blunt end of an adjacent teardrop (sT>B jump), while the remaining 19% of the jumps were head-on from the blunt end of a teardrop to tip of an adjacent teardrop (hB>T jump). Even slight alteration of island placement to Pattern B (**Fig. 1B** and **Movie 2**) eliminated this bias. On Pattern B, 60% of the jumps were observed to be sideways from the blunt end of a teardrop to the tip of an adjacent teardrop (sB>T jump), while the remaining 40% of the jumps were head-on from the tip of a teardrop to the blunt end of an adjacent teardrop (hT>B jump). Patterns lacking asymmetric islands (**Fig. 1C**), gap size (**Fig. 1D, E**) or both (**Fig. 1F**) also exhibited no bias. Thus, only Pattern A exhibited strong directional bias, demonstrating that gap size, teardrop asymmetry and the relative positioning of the teardrops are all essential features.

We have observed the same directional bias in normal human epidermal keratinocytes (NHEK) migrating on similar patterns (**Fig. S1**). It is noteworthy that the directional bias observed here differs from that reported in the previous study involving 3T3 fibroblast and human microvascular endothelial cell (HMVEC) movement on teardrop micropatterns.[2] This difference may be attributed to disparate cell migration properties of mesenchymal versus epithelial cell types (**Fig. S2**) and the significantly different environmental signals, including growth factors and extracellular matrix (ECM) proteins, to which cells were exposed. That different cell types exhibit distinct movement tendencies is expected and has been documented, for example, in tumor cells with different requirements for extracellular proteolysis.[9] The key question of interest here is whether and how the movement bias can be rationally re-programmed by modulating micropattern features and key cellular signals.

3.2. Geometrical modification based on quantitative jump analysis enhances directional bias

Based on our quantitative measurements of cell movement on teardrop squares, we sought to design a new pattern that enhances the directional bias. The preference for sT>B jumps on Pattern A (Fig. 1A) was only 80% with the other 20% involving hB>T jumps. We reasoned that the bias for sT>B jump may be further enhanced if this jump option were juxtaposed against an even more unfavorable type of jump. One possibility for a highly unfavorable jump came from the observations of cell movement on Pattern B (Fig. 1B). Cell movement on Pattern B was not only unbiased, but also the frequency of jumps was significantly lower than on Pattern A (**Table S1**). These observations suggested that the hB>T and sT>B jumps are highly unfavorable and could be ideal candidates to juxtapose against the highly favored sT>B jump from Pattern A.

Thus, we designed a new yin-yang pattern that juxtaposed the sB>T jump against the sT>B jump and where only sideway jumps are possible (sB>T or sT>B jumps; **Fig. 1G**). As a control, we designed another yin-yang pattern where only head-on jumps are possible (**Fig. 1H**) at both ends of the curved teardrop. Consistent with our hypothesis, the sideways yin-yang pattern resulted in an enhanced T>B directional bias (91%; **Movie 3**) compared to the original Pattern A in which the T>B directional bias was 80%. In contrast, the control head-on yin-yang pattern yielded little bias in cell movement.

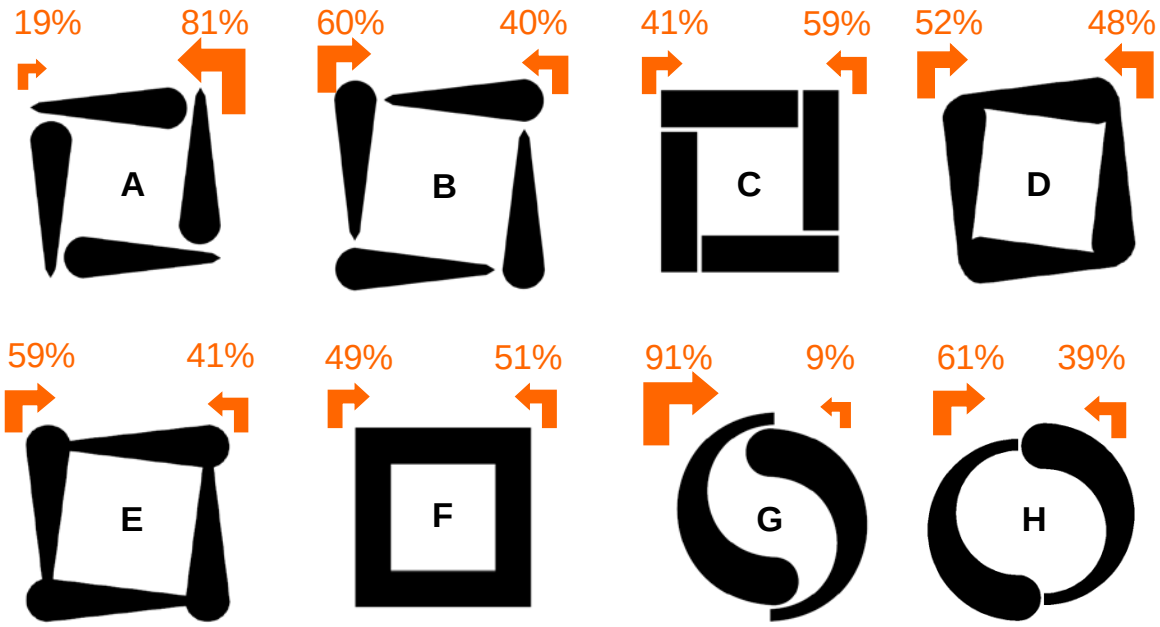

Figure 1. Directional bias of MCF-10A epithelial cells on teardrop-based micropatterns. Standard dimensions for the adhesive islands were 20 μm in width and 80μm in length with 3μm non-adhesive gaps between islands. The width of the teardrop is 3 μm at the tip and 20 μm at the blunt end. The patterns are: (**A**) disjointed teardrops with the blunt end running into a tip, (**B**) disjointed teardrops with tip running into the blunt end, (**C**) disjointed adhesive islands lacking asymmetry, (**D**) Pattern A without gaps, (**E**) Pattern B without gaps, (**F**) pattern with both gaps and island asymmetry eliminated, (**G**) sideways yin-yang pattern and (**H**) head-on yin-yang pattern. Percentages of complete jumps in each direction are shown (greater than 100 jumps quantified for each pattern).

3.3. Signal alteration based on lamellipodial observations flips directional bias

In addition to using quantitative analysis of movement tendencies to engineer patterns with enhanced directional bias, we sought to better understand the preference that epithelial cells exhibit for the sT>B jump as opposed to the sB>T jump or the head-on alternatives. We examined more closely the sT>B jump at 63x magnification. On Pattern A, we noticed that as the lamellipodium of a moving cell becomes constrained at the tip end of a teardrop, the cell extends a new side lamellipodium that is stabilized by latching onto a lateral island (**Fig. 2A** and **Movie 4**). In sharp contrast, Pattern B does not provide a lateral island to stabilize a new side lamellipodia; thus, in order to jump onto an adjacent island, cells encountering a tip on Pattern B must use their pre-existing spatially-constrained lamellipodia to reach out in a headlong direction (**Movie 5**). Thus, high directional bias seems to be the consequence of side lamellipodial protrusions at the tip ends that are stabilized by adhesions to a lateral, adjacent island.

This observation of side lamellipodium formation suggested that the bias of the cells on these micropatterns may be sensitive to intracellular signals that control lamellipodial extensions, such as Rac1, a small GTPase signaling protein. Specifically, moderate Rac1 knockdown has been shown to reduce the formation of new lamellipodia and increase the directional persistence of cells on non-patterned tissue culture substrates.[10] Thus, we reasoned that moderate Rac1 suppression may enhance the stability of a pre-existing lamellipodium and thereby improve the ability to make head-on jumps instead of switching direction via a sideways jump.

To test this hypothesis, we suppressed the expression level of Rac1 by ~60% using RNA interference (**Fig. S3**). MCF-10A cells with reduced Rac1 expression exhibited a different motility bias compared to cells transfected with control siRNA (**Fig. 2B**). Rac1 suppression significantly reduced the bias for sT>B jumps in Pattern A (90% to 61%; Fig. 2B and **Movie 6**) and increased the bias for hT>B jumps in Pattern B (53% to 80%; Fig. 2B and **Movie 7**). By discouraging sideways jumps and promoting head-on jumps, we dampened the biased movement on Pattern A and created a new bias on the previously ineffective Pattern B. Conferring this new bias in movement comes with an expected cost in the speed of cell movement: due to dampened lamellipodial activity in cells transfected with Rac1 RNAi, the speed of migration and frequency of jumps were reduced. These results demonstrate that the directional bias of cell motility on micropatterned surfaces may be re-programmed by tuning an intracellular signal that regulates lamellipodial extensions.

It is noteworthy that attenuating Rac1 expression enhances the tendency of cells to hop in a direction parallel to the major axis of the teardrop. On Pattern B, the preference for hops parallel to the teardrop axis (hT>B jump) increases from 53% (control siRNA) to 80% (Rac1 siRNA). The result is a movement bias that closely resembles that reported previously for fibroblasts and HMVEC on similar patterns.[2] On Pattern A, Rac1 suppression has a similar effect although the conversion is not complete: the preference to hop parallel to the major axis of the teardrop (hB>T jump) increases from 10% (control siRNA) to 39% (Rac1 siRNA). These results are consistent with our hypothesis that partial suppression of Rac1 stabilizes pre-existing lamellipodia, thereby enhancing the ability to make headlong jumps. It also suggests that Rac1 level may be a

molecular determinant of the observed differences in the movement preference of fibroblasts/HMVEC versus epithelial cells and may serve as a quantitative index to predict the movement of other cell lines on micropatterns

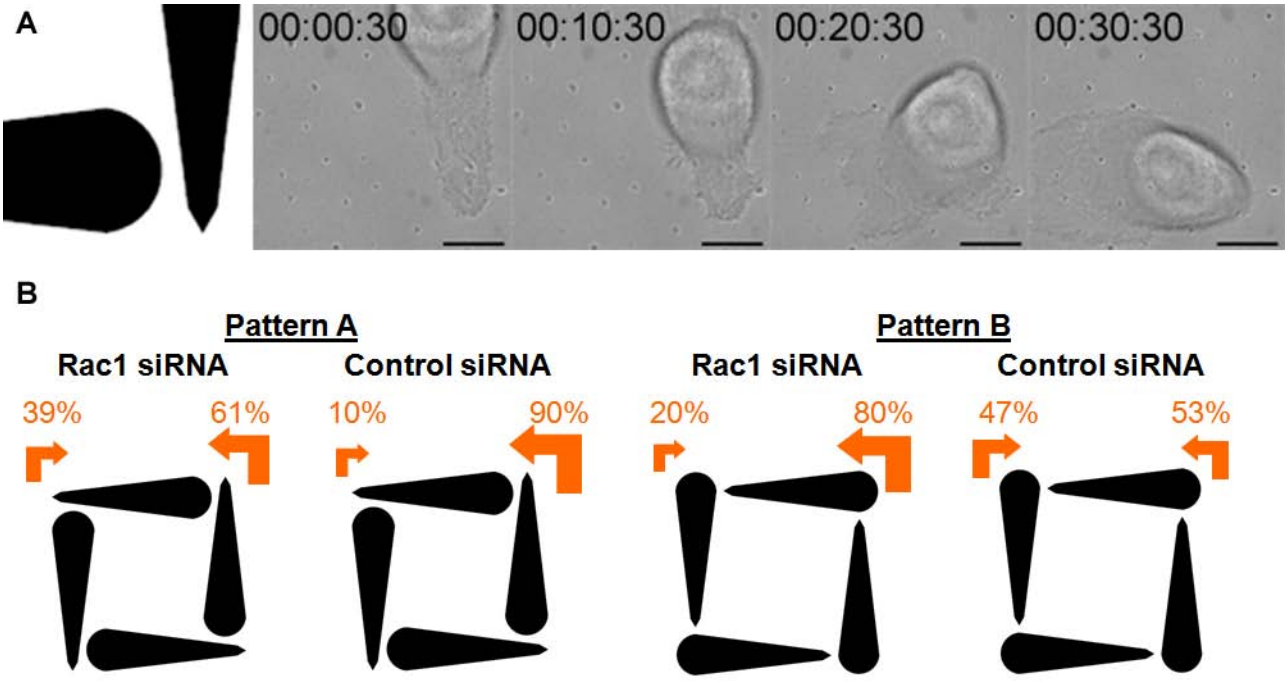

Figure 2. The role of lamellipodial extensions in determining the directional bias of cell movement on micropatterns. (**A**) Timelapse images show the formation of a new, side lamellipodium as a cell jumps sideways from the tip to a blunt end on Pattern A. The corner of Pattern A at which the cell is jumping is shown in the first panel. The time stamps correspond to Movie 4, displayed in h:min:s. (**B**) The effect of Rac1 knockdown on the directional bias of MCF-10A cells on micropatterned surfaces. Directional bias of Rac1 siRNA-treated and control siRNA-treated cells on Pattern A and Pattern B are

shown. Percentages of complete jumps in each direction are shown (greater than 100 jumps quantified for each pattern).

3.4. Novel splitter design modulates cell flux

In addition to re-programming the directional bias, it is desirable to tune the flux of cell movement on synthetic materials. To explore this possibility, we adapted the aforementioned teardrop micropatterns into a "splitter" design (**Fig. 3A**). Cells originating in the source island (S) would jump to one of the available lateral target islands (T1 and T2). We reasoned that by varying the position of T2, the relative flux of cells moving to T1 versus T2 may be modulated. Thus, we designed micropatterns with the relative position of S and T1 fixed while varying the gap distance or the position offset of T2.

These splitter features have qualitatively distinct effects. Cell movement is highly sensitive to gap distance, displaying a switch-like transition as the gap distance is shifted from 3 to 5 μm (**Fig. 3B**). On the other hand, position offset provided a graded transition as the offset is increased from 0 to 15μm (**Fig. 3C**). Cells had a higher likelihood of jumping to T1 with no offset, and this bias can be gradually increased to near 100% by increasing the offset of T2. These results suggest that varying the offset can be useful in modulating the relative flux of cells along two micropatterned lanes emanating from a splitter design.

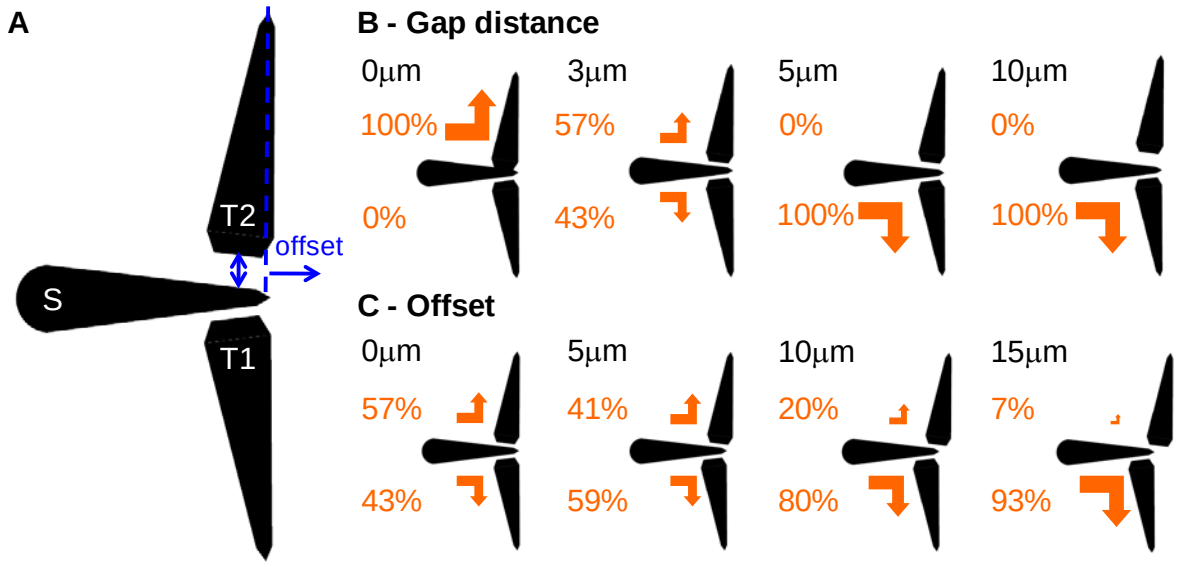

Figure 3. The effect of splitter design features on the directional bias. (**A**) Cells jumping from the source island (S) to adjacent target islands (T1 or T2) were counted. While the positions of S and T1 were held fixed, (**B**) the gap distance and (**C**) the position offset of T2 were varied. Percentages of complete jumps in each direction are shown (greater than 100 jumps were quantified for each pattern).

4. Conclusion

An emerging property of micropatterned surfaces is their ability to orient cell movement.[1-3] Our signal perturbation experiments along with quantitative analysis of cell movement tendencies reveal a key role for lamellipodial extensions and stabilization in determining the directional bias of epithelial cells on micropatterned surfaces. Manipulating pattern features and cellular signals to exploit and modulate lamellipodial

extensions enables both quantitative tuning and qualitative re-programming of the directional bias of cell movement. These findings provide a foundation for modulating the direction and flux of epithelial cell movement on micropatterned surfaces as a powerful complement to gradient-based approaches.[11-13] Together with similar studies focused on other cell types, we envision developing a complete toolbox for programming cellular traffic on micropatterned surfaces for applications, such as tissue engineering.

5. Experimental Methods

5.1. Fabrication of micropatterned substrates

Microcontact printing with a polydimethylsiloxane (PDMS) stamp was used to pattern the adhesion ligand, fibronectin, onto a gold-coated coverslide. Briefly, the PDMS stamp is micro-fabricated using the standard photolithographic techniques [14]; UV light is passed through a chrome mask containing the pattern (Nanoelectronics Research Facility, UCLA) onto a layer of SU-8 photoresist to make a mold, onto which PDMS is cast to make the stamp. The stamp is then "inked" with 16-Mercaptohexadecanoic acid (Sigma Aldrich) dissolved in 99% ethanol and used to print the pattern onto a gold-coated chambered coverslide (Labtek). The unprinted area is passivated using PEG(6)-Thiol (Prochimia) dissolved in 99% ethanol to prevent non-specific binding of cells. After washing with PBS twice, EDC and Sulfo-NHS (Pierce) dissolved in PBS is added to the coverslide to activate the acid to crosslink covalently with the amine group of the subsequently added fibronectin (Sigma Aldrich) dissolved in PBS at 10μg/mL. Finally, BSA conjugated with Alexa Fluor 594 (Invitrogen) was doped into the fibronectin solution for the purpose of pattern visualization (**Fig. S4**).

5.2. Cell culture

MCF-10A human epithelial cells were cultured in growth medium composed of Dulbecco's modified Eagle's medium/Ham's F-12 containing HEPES and L-glutamine (DMEM/F12, Invitrogen) supplemented with 5% horse serum (Invitrogen), 1% penicillin/streptomycin, 10 µg/mL insulin (Sigma), 0.5 µg/mL hydrocortizone (Sigma), 20ng/mL EGF (Peprotech) and 0.1 µg/mL cholera toxin (Sigma) and maintained under humidified conditions at 37ºC and 5% CO_2. Cells were passaged regularly by dissociating confluent monolayers with 0.05% trypsin-EDTA (Invitrogen) and suspending cells in DMEM/F12 supplemented with 20% horse serum and 1% penicillin/streptomycin. After two washes, cells were diluted 1:4 and plated in growth medium.

5.3. Time-lapse microscopy

Cells were seeded in growth medium for 1 hr onto the micropatterned substrate. After washing to remove non-adherent cells, the culture was incubated with fresh growth medium for 1 hr and imaged at 10x magnification every 5 min for 12 hr or at 63x magnification every 30 sec for 2 hr. For siRNA-treated cells, the seeding time was increased by 2 hours. Cells were maintained at 37ºC and 5% CO_2 in a heated chamber with temperature and CO_2 controller (Pecon) during time-lapse imaging. Images and movies were acquired using Axiovert 200M microscope (Carl Zeiss), and Axio Vision LE Rel. 4.7 (Carl Zeiss) was used for image analysis.

5.4. siRNA knockdown

siRNA targeting human Rac1 mRNAs (siGENOME SMARTpool, M-003560-06-0005) and non-targeting siRNA (siGENOME Non-Targeting siRNA pool #2, D-001206-14-05) were obtained from Thermo Scientific. Cells were transfected with 20 nM siRNA using lipofectamine RNAiMAX 2000 (Invitrogen).

6. Acknowledgements

We thank the members of the Asthagiri group for helpful discussions. This research was funded by the NSF Center for Science and Engineering of Materials at Caltech. We also gratefully acknowledge the technical support and infrastructure provided by the Kavli Nanoscience Institute. Supporting Information is available online from Wiley InterScience or from the author.

7. References

[1] X. Jiang, D. A. Bruzewicz, A. P. Wong, M. Piel, G. M. Whitesides, *Proc Natl Acad Sci U S A* **2005**, *102*, 975.

[2] G. Kumar, C. C. Ho, C. C. Co, *Advanced Materials* **2007**, *19*, 1084.

[3] G. Mahmud, C. J. Campbell, K. J. M. Bishop, Y. A. Komarova, O. Chaga, S. Soh, S. Huda, K. Kandere-Grzybowska, B. A. Grzybowski, *Nature Physics* **2009**, *5*, 606.

[4] C. S. Chen, M. Mrksich, S. Huang, G. M. Whitesides, D. E. Ingber, *Science* **1997**, *276*, 1425.

[5] R. McBeath, D. M. Pirone, C. M. Nelson, K. Bhadriraju, C. S. Chen, *Developmental Cell* **2004**, *6*, 483.

[6] R. Singhvi, A. Kumar, G. P. Lopez, G. N. Stephanopoulos, D. I. C. Wang, G. M. Whitesides, D. E. Ingber, *Science* **1994**, *264*, 696.

[7] D. A. Lauffenburger, A. F. Horwitz, *Cell* **1996**, *84*, 359.

[8] A. J. Ridley, M. A. Schwartz, K. Burridge, R. A. Firtel, M. H. Ginsberg, G. Borisy, J. T. Parsons, A. R. Horwitz, *Science* **2003**, *302*, 1704.

[9] K. Wolf, I. Mazo, H. Leung, K. Engelke, U. H. von Andrian, E. I. Deryugina, A. Y. Strongin, E. B. Brocker, P. Friedl, *Journal of Cell Biology* **2003**, *160*, 267.

[10] R. Pankov, Y. Endo, S. Even-Ram, M. Araki, K. Clark, E. Cukierman, K. Matsumoto, K. M. Yamada, *Journal of Cell Biology* **2005**, *170*, 793.

[11] S. B. Carter, *Nature* **1965**, *208*, 1183.

[12] C. M. Lo, H. B. Wang, M. Dembo, Y. L. Wang, *Biophys J* **2000**, *79*, 144.

[13] J. Y. Wong, A. Velasco, P. Rajagopalan, Q. Pham, *Langmuir* **2003**, *19*, 1908.

[14] S. Raghavan, C. S. Chen, *Advanced Materials* **2004**, *16*, 1303.

8. Supporting Information

8.1. Supporting figures

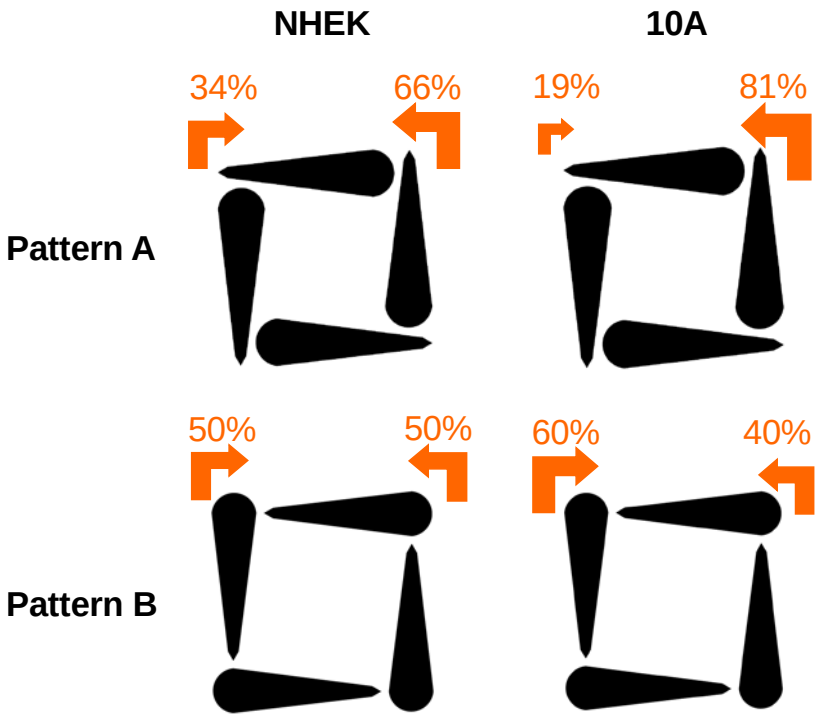

Figure S1. Directional bias of normal human epidermal keratinocytes (NHEK) on Patterns A and B. The directional bias for MCF-10A epithelial cells (right column) is also displayed.

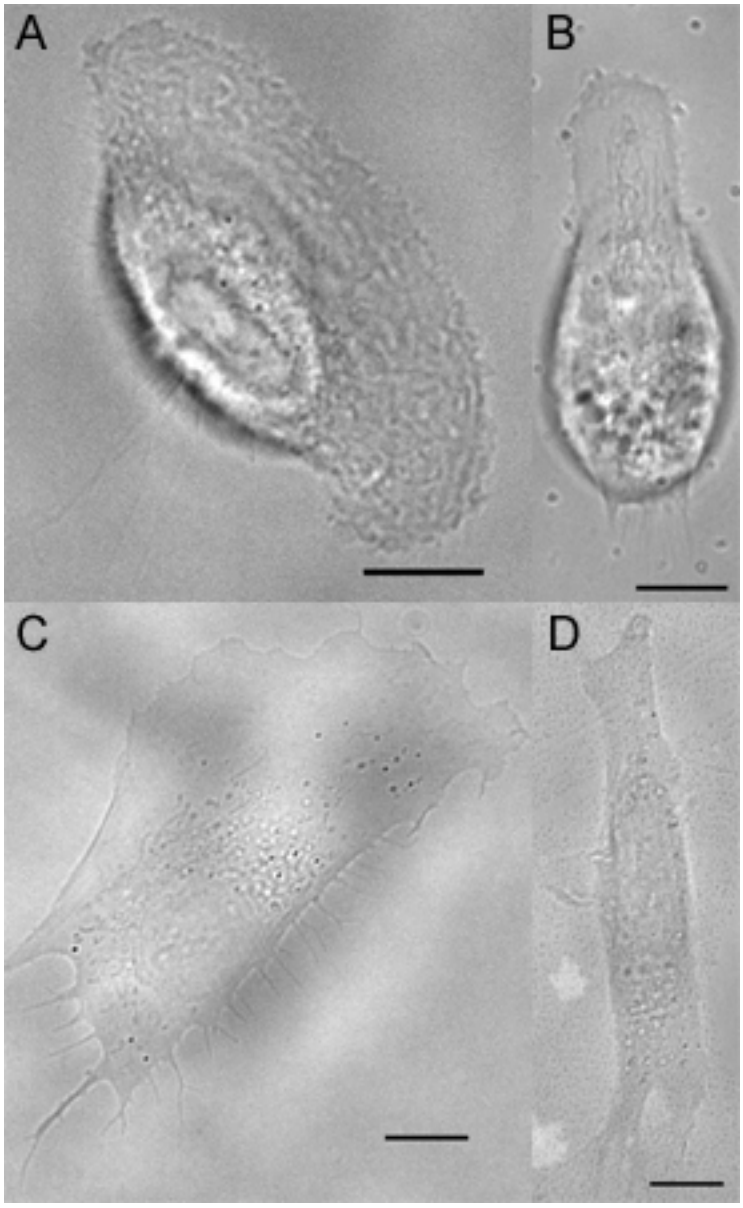

Figure S2. Morphology of migrating MCF-10A epithelial cells and Rat1 fibroblasts. MCF-10A cells on (**A**) uniform, non-patterned surface exhibit a clear, broad lamellipodium, while cells on (**B**) 10μm line pattern exhibit a highly motile morphology with a lamellipodium constrained by the width of the micropattern. In sharp contrast, Rat1 fibroblasts on (**C**) uniform, non-patterned surface exhibit multiple lamellipodia,

while fibroblasts on (**D**) 10μm line pattern exhibit a less motile morphology with active lamellipodia on two ends despite the constraints by the width of the micropattern. Scale bar, 10μm.

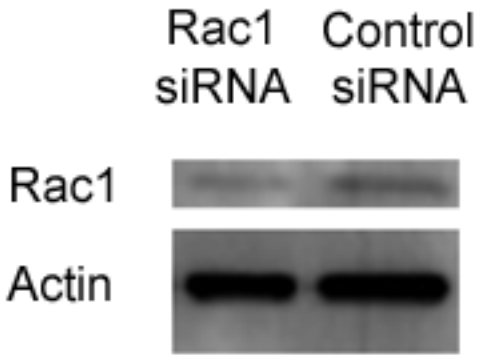

Figure S3. Effect of RNA interference on Rac1 expression level. Western blot image of Rac1 siRNA knockdown. Concentration of siRNA was 20nM and Rac1 expression level was reduced to 40% of the control, as quantified by Versadoc Imaging System.

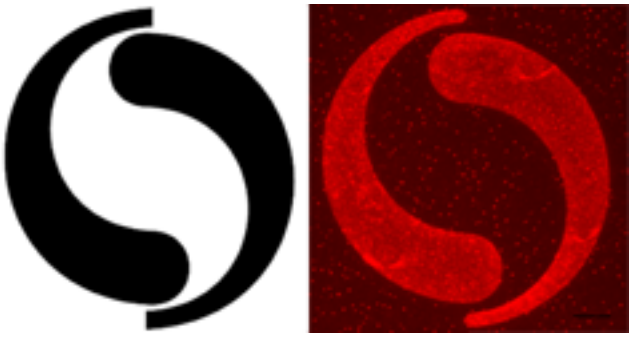

Figure S4. Fluorescence imaging of the underlying micropattern via BSA-Cy3. Scale bar, 10μm.

8.2. Supporting table

Table S1. Detailed analysis of the jumps of MCF-10A epithelial cells from either blunt or tip ends over two experiments. Note that cells on pattern B jump less successfully.

	Blunt End			**Tip End**		
	Successful Attempts [a]	Unsuccessful Attempts [b]	No Visible Attempts [c]	Successful Attempts	Unsuccessful Attempts	No Visible Attempts
Pattern A	31	13	66	165	24	61
Pattern B	13	9	25	9	6	29

[a] Successful attempt corresponds to a complete translocation of cells from one island to the other. [b] Unsuccessful attempt corresponds to a failed lamellipodial extension to an adjacent island which subsequently retracts. [c] No visible attempt corresponds to a reversal of movement direction without any attempt to jump to an adjacent island.

8.3. Movie legends

Movie 1. MCF-10A cell migrating with high bias on Pattern A. This pattern is depicted in Fig. 1A and in the first frame of this movie. Images were acquired every 5 min for 8.6 h (103 frames) and compiled at 10 frames/s in the movie. Scale bar, 20μm.

Movie 2. MCF-10A cell migrating with low bias on Pattern B. This pattern is depicted in Fig. 1B and in the first frame of this movie. Images were acquired every 5 min for 12 h (144 frames) and compiled at 10 frames/s in the movie. Scale bar, 20μm.

Movie 3. MCF-10A cells migrating with high bias on sideways yin-yang pattern. This pattern is depicted in Fig. 1G and in the first frame of this movie. This movie shows two cells moving on two separate yin-yang patterns (top and bottom). Images were acquired every 5 min for 12 h (144 frames) and compiled at 10 frames/s in the movie. Scale bar, 20μm.

Movie 4. Formation of new, side lamellipodia when jumping from the tip to a blunt end on Pattern A (63x magnification). Images were acquired every 30 s for 0.7 h (81 frames) and compiled at 10 frames/s in the movie. The first frame shows the region of the micropattern on which the cell is moving. Scale bar, 10μm.

Movie 5. Lack of new, side lamellipodia when jumping from tip end on Pattern B (63x magnification). Images were acquired every 30 s for 0.8 h (101 frames) and compiled at 10 frames/s in the movie. The first frame shows the region of the micropattern on which the cell is moving. Scale bar, 10μm.

Movie 6. Rac1 siRNA-treated MCF-10A cell with reduced bias on Pattern A. This pattern is depicted in Fig. 1A and in the first frame of this movie. Images were acquired every 5 min for 12 h (144 frames) and compiled at 10 frames/s in the movie. Scale bar, 20μm.

Movie 7. Rac1 siRNA-treated MCF-10A cell with increased bias on Pattern B. This pattern is depicted in Fig. 1B and in the first frame of this movie. Images were acquired every 5 min for 10.8 h (130 frames) and compiled at 10 frames/s in the movie. Scale bar, 20μm.

Chapter III: A Hybrid Micropattern Design for Supra-Oriented Cell Movement and Enhanced Multicellular Partitioning

1. Abstract

Geometrical constraints imposed by micropatterns affect cell motility. Micropatterned lines polarize cells and confine cell movement along a single axis.[1, 2] More recently, these line patterns have been shown to improve cell speed albeit the direction in which cells move along the line cannot be controlled.[3] Meanwhile, we and others have shown that teardrop-shaped micropatterns provide control over the direction of cell migration.[4, 5] As we begin to understand how specific micropatterned geometries affect cell motility, an emerging challenge is to mix and match pattern geometries to achieve multifaceted improvements in cell motility. Here, we show that the enhanced speed and persistence provided by line micropatterns and the directional control provided by the teardrop geometry may be combined in a new hybrid design to achieve rapid, directed cell movement. The hybrid micropattern increased the persistence and directional bias of cell movement compared to the standard teardrop geometry, revealing that combining geometric features can lead to unexpected synergistic improvements in cell motility. Using the hybrid micropattern as a polar bridge between two reservoirs, we show that cells may be selectively partitioned to one reservoir with approximately 85% enrichment within 36 hr.

2. Introduction

Physical cues from the surrounding environment can dictate cellular motility. For example, cancer cells can reorient surrounding ECM into parallel fibers that radiate outward from the tumor explants and can migrate along these fibers to facilitate metastasis.[6] Furthermore, there is emerging evidence that physically constrained environments, such as the blood and lymphatic vessels, promote cancer metastasis as well.[7] Researchers have tried to mimic such environments through micropatterning, and one such example is the line pattern.

Micropatterned lines have been used to guide axonal growth in neurons, aid blood vessel-like tissue formation, and study auto-reverse nuclear migration.[8-10] More recently, Yamada and colleagues found that cells on line patterns with sub-cellular widths can establish a uniaxial morphology with enhanced cell speed (unilamellar morphology).[3] However, if the lanes were too narrow, cell migration was hampered, and thus there was an optimum lane width for maximum cell speed.

Line patterns, however, do not permit control over the direction of cell movement. On the other hand, we and others have shown that teardrop-based micropatterns can be used to program the direction of cell movement.[4, 5] As we begin to understand better how micropattern features affect cell migration properties, it is intriguing to probe whether pattern features can be mixed and matched to achieve combinatorial enhancements in directed cell migration. Here, we sought to test whether a hybrid pattern that combines line and teardrop features might enable both rapid and directed movement.

3. Results

3.1. Line patterns markedly enhance persistence in addition to cell speed

To begin to design our hybrid pattern, we first quantified cell movement of MCF-10A epithelial cells on micropatterned lines of different widths to determine the optimum line width for maximum cell speed. Consistent with previous studies,[3] we observed that the majority of MCF-10A cells established a migratory morphology with a single prominent lamella on one side of the cell when seeded on line patterns (unilamellar morphology; Chapter II Figure S2B). The cells moved ~40-50% faster on micropatterned lines than their counterparts on non-patterned surfaces that were prepared with identical chemistry (**Table 1**). The maximum cell speed was observed at an intermediate line width of 20 μm, above which the cells could no longer maintain the unilamellar morphology due to the lack of constraints at a single-cell width. The cells on thicker lines (30 μm and up) did not exhibit migration speed nor persistence length statistically different from that of non-patterned surface. Consistent with previous study with other cell lines,[3] there is an optimum width for maximum speed and it is 20 μm for MCF-10A cells.

Interestingly, we also observed significantly enhanced persistence upon confining MCF-10A cells to line patterns compared to cells on non-patterned surfaces. The cells with unilamellar morphology moved approximately 250-300 μm before flipping direction. In contrast, cells on a non-patterned surface moved only 50 μm on average before changing direction. As with cell speed, the optimum persistence length was observed on 20 μm-thick lines. Taken together, our observations show that both persistence and

migration speed enhancements correlate with the establishment of the unilamellar morphology.

	Non-pattern	Line (5 μm)	Line (10 μm)	Line (20 μm)	Line (30 μm)
Average persistence length (μm)	54 [12]	253 [40]	256 [57]	310 [65]	98 [41]
Average migration speed (μm/hr)	55.5 [8.3]	81.1 [12.0]	87.4 [11.3]	98.8 [14.7]	60.9 [12.9]
Fraction cells exhibiting unilamellar morphology	0%	96%	96%	92%	4%

Table 1. Enhanced motility of MCF-10A epithelial cells on line patterns. Both the persistence length and cell migration speed are enhanced on line patterns, and are maximized on the thickest line. Unilamellar morphology was only observed on line patterns with widths below 20 μm. Persistence length is the distance cells travel before changing the direction 180° or breaking unilamellar morphology to spread. Migration speed includes the time they take to change directions. Values in the square brackets indicate standard error of the mean (n = 2-4).

3.2. A hybrid micropattern design that combines line and teardrop features

Although the 20μm line pattern provides significant enhancements to the speed and persistence of MCF-10A cell migration, this micropattern geometry provides no

control over the direction in which the cell travels. That is, the physical constraint imposed by the line geometry dramatically increases the tendency of cells to *maintain* a direction but does not bias cells to move preferentially up or down the line. In contrast, we and others have shown that teardrop-shaped micropatterns impart a directional bias to cell movement.[4, 5] MCF-10A cells preferentially hop from the tip end of a teardrop onto the blunt end of an adjacent island, leading cells to move in the counterclockwise direction (**Figure 1A**).

An intriguing hypothesis is that the effect of micropattern geometry on cell migration is modular. Such modularity would allow one to mix and match different micropattern shapes to achieve combinatorial enhancements in cell migration. To test this hypothesis, we designed a hybrid micropattern that blended the features of the line and teardrop geometries and quantitatively analyzed cell migration on this hybrid micropattern.

The hybrid design involved the insertion of a line segment of the optimum width (20 μm) between the blunt and tip ends of the standard teardrop pattern (**Figure 1B**). The hybrid design yields a spear-shaped pattern that maintains the blunt and tip ends, as these features were previously shown to play a key role in determining the directional bias with which cells hop from one micropatterned island to the next. Having hopped onto an island, cells would have to traverse the middle line segment to reach the other end. Since cells migrate with high persistence on line patterns, we reasoned that cells would successfully migrate across the line segment without turning back, provided that the length of the segment was significantly lower than the persistence length of cell

migration on line patterns (300 µm). Thus, the length of middle line segment was set at 100 µm.

To assess the effect of the hybrid micropattern on cell motility, we analyzed and compared the migration of MCF-10A cells on spear-shaped versus teardrop-shaped micropatterned islands. Both micropatterned islands were arranged to form a square-shaped "track" around which cells migrate. To ensure that any observed differences in migration could be attributed solely to the shape of the micropatterned island, the islands were arranged with precisely the same spacing and relative positioning. Time-lapse images were acquired of individual MCF-10A cells migrating on the square tracks, and the directional bias, persistence and speed of MCF-10A cell movement were quantified.

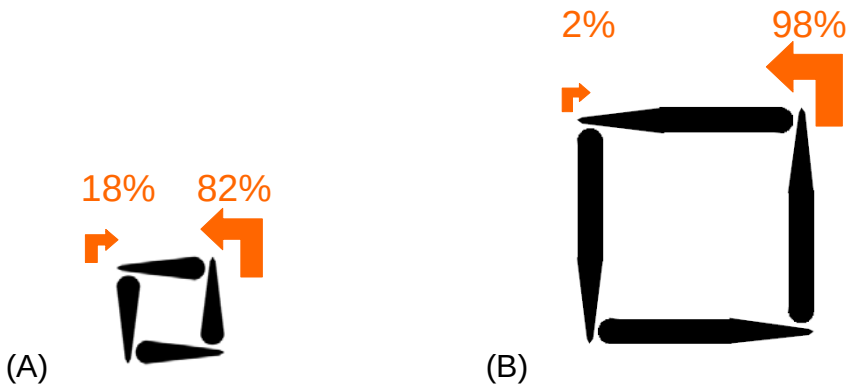

Figure 1. Schematic and directional bias of (A) teardrop and (B) spear-shaped patterns. Directional bias of spear-shaped patterns is greatly enhanced compared to the original teardrop patterns. Spear-shaped pattern has an extra 100 µm long, 20 µm wide line segment insertion in each of the teardrop islands (originally 80 µm long and 20 µm wide at blunt end).

3.3. The hybrid spear-shaped micropattern markedly improves the directional bias of cell movement

We first confirmed that the directional bias of cell migration exhibited on the original teardrop micropattern was not compromised by the addition of the middle line segment. Unexpectedly, cell migration on the hybrid spear-shaped micropattern exhibited even greater directional bias than on the original teardrop design. On the spear micropattern, cells moved from island to island with 98% of the hops favoring the blunt-to-tip direction, while only 2% of the successful hops occurred in the tip-to-blunt direction (**Figure 1B**). Meanwhile, on the standard teardrop-shaped micropattern, the bias for the blunt-to-tip hops was only 82% (**Figure 1A**).

To better understand this unexpected improvement in directional bias, we quantified the "decision" that cells make at each end of the spear- and teardrop-shaped micropatterns. On each end (tip or blunt), we quantified the likelihood that a cell hops to the adjacent island (successful hop) as opposed to "bouncing" by turning back to migrate down the island (**Table 2**). On the tip end of teardrop micropatterns, the hop probability was 73%. In contrast, the hop probability improved to 97% on the tip end of spear-shaped micropatterns. Furthermore, the likelihood that a cell hopped on the blunt end decreased from 38% on teardrop patterns to 15% on the hybrid spear patterns. Thus, the inclusion of a middle line segment in the teardrop pattern not only improved the likelihood of a hop at the tip end, but also reduced the probability that a cell would hop at

the blunt end. Thus, improvements in cell fate choices at both ends of the spear pattern together yield a marked enhancement in the directional bias of cell movement.

Events at Corners	Occurrences for Teardrop	Occurrences for Spear	Average Residence Time for Teardrop (min)	Average Residence Time for Spear (min)
Successful hop at tip end	208 (51.5%)	166 (83.4%)	30.7	28.5
Successful hop at blunt end	45 (11.1%)	4 (2.0%)	39.9	26.7
Bounce at tip end	78 (19.3%)	6 (3.0%)	48.9	28.5
Bounce at blunt end	73 (18.1%)	23 (11.6%)	50.6	41.4

Table 2. Detailed analysis of hop decisions at corners and residence times associated with the events. Events at each corner of the islands reveal the enhanced directional bias on the spear-shaped patterns. Residence times between the two patterns were statistically not different (except for residence time for bounce at tip end).

3.4. Hybridizing line and teardrop micropatterns yields an additive improvement in the persistence of cell migration

In addition to directional bias, our quantitative analysis showed that the tendency of cells to maintain the direction of movement increased on the hybrid spear micropattern compared to the original teardrop pattern. The average distance cells moved before

changing direction on the teardrop patterns was 383 μm. On the spear-shaped micropattern, the persistence length increased by 141% to 925 μm (**Table 3**). The observed increase in persistence was approximately equal to that expected by hybridizing a line segment and a teardrop pattern. Inserting a 100 μm line segment in an 80 μm teardrop would be expected to increase, the persistence by 125% to 862 μm, a value that differs only by 7% from the measured persistence of 925 μm. These results reveal that the line and teardrop shapes provide modular benefits to the persistence of cell migration, such that a hybrid pattern yields an approximately additive and predictable improvement in this aspect of cell migration.

Speed and Persistence	**Teardrop**	**Spear**
Average persistence length (μm) [a]	383 [230]	925 [295]
Average speed (μm/hr) [b]	91.0 [14.4]	121.3 [14.2]
Average net speed in the preferred direction (μm/hr) [c]	39.3 [31.6]	92.9 [41.4]

[a] Average persistence length corresponds to the average of distances cells traveled in the preferred direction without changing direction. [b] Speed corresponds to the total distance traveled divided by the total time. [c] Net speed corresponds to the net distance in preferred direction (distance in preferred direction – distance in opposite direction) divided by the total time.

Table 3. Cell motility on teardrop patterns and spear-shaped patterns. Speed and persistence are significantly enhanced on the spear-shaped patterns when compared to teardrop patterns. The differences between spear-shaped patterns and teardrop patterns

were statistically significant for all three parameters ($p < 0.01$; $n = 3$, more than 40 cells analyzed for each pattern). Values in the square brackets indicate standard error of the mean ($n = 2$-4).

3.5. Reduced frequency of hops lead to improvements in migration speed on spear-shaped micropatterns

Finally, we assessed the effect of inserting a line segment into the teardrop micropattern on cell migration speed. Since cell speed on line patterns is similar to that on teardrop patterns (98.8 on line and 91.0 μm/hr on teardrop), inserting a line segment into the teardrop pattern was not expected to affect cell migration speed. Quantitative analysis of time-lapse videos, however, revealed that the average cell speed on spear-shaped micropatterns was 121 μm/hr, a 33% improvement compared to teardrop micropatterns (**Table 3**).

To better understand this unexpected improvement in cell speed, we examined more closely the events at the corners of the square track where cells hop from one island to the next. We reasoned that the spear-shaped pattern may improve the average migration speed by reducing the amount of time for cells to hop at each corner. To test this possibility, we quantified the residence time of cells at the corners of the square track during tip-to-blunt and blunt-to-tip hops (**Table 2**). Residence times on spear-shaped patterns were on average shorter than those on teardrop patterns. The average residence times spent at the tip end were 29 min and 40 min on spear and teardrop patterns, respectively, while the times spent at the blunt end were 34 min and 46 min on spear and

teardrop patterns, respectively. Further analyses, however, showed these differences in hop duration were not statistically significant. Also, the residence times for U-turns were on average greater than residence times for successful hops at both ends of the island, but were mostly statistically not significant. These results revealed that the residence times at the corners of the square track were not statistically different between spear and teardrop patterns.

While differences in residence times do not contribute to the improvement in cell speed on spear patterns, this analysis raised an alternate hypothesis. With hops taking on average 37 min on spear and teardrop patterns, it consumes a significant fraction of the time a cell spends in traversing around the square track. For example, on a teardrop pattern, the cell takes 3.5 hr to traverse the track (320 μm ÷ 91 μm/hr) of which 2.8 hr is spent hopping at the corners. This observation taken together with the fact that hops occur more frequently on teardrop patterns (owing to their shorter length) may explain the improvement in average migration speed on spear shaped patterns.

To analyze this idea more quantitatively, we note that on the teardrop pattern, a hop decision must be made every 80 μm; in contrast, on the spear-shaped pattern, these decisions are spaced further apart (180 μm). Thus, the frequency of hops is approximately two fold greater on teardrop patterns. If we hypothetically insert an extra hop along a spear-shaped pattern, then the transit time along the spear would increase by 37 min or 0.6 hr from 180 μm ÷ 121 μm/hr = 1.5 hr to 2.1 hr. With this correction for hop frequency, the adjusted speed on spear-shaped patterns becomes 180 μm ÷ 2.1 hr =

86 μm/hr, a value that nearly matches the speed observed on teardrop-shaped pattern (91 μm/hr).

Therefore, we conclude that the hybrid spear-shaped micropattern improves cell migration speed not by enhancing cell migration or reducing the time it takes for cells to hop, but rather by requiring fewer hops per unit length owing to the insertion of a line segment in the base teardrop pattern. By inserting a line segment into the classical teardrop pattern, we exploit the remarkably high persistence of cell migration on line patterns. Thus, the directional bias conferred by each hop is capitalized over longer linear runs before the next junction is required to re-establish and maintain the bias in movement.

3.6. Micropatterned bridges with hybrid patterns result in a rapid and effective partitioning across long distances

As a step towards an application-oriented, high-order pattern to control cell population, we converted the highly biased spear-shaped patterns into a partition design. The spear-shaped patterns were extended in a zigzag fashion to bridge the two chambers separated by a 1000 μm distance (**Figure 3A**; note that the actual total distance of the spear-shaped bridge is 1500 μm long) and teardrop patterns were similarly converted into a bridge for comparison (**Figure 3B**; total distance of the teardrop bridge is 2268 μm long), while a simple straight line was used to connect the chambers for the control pattern (**Figure 3C**). We investigated the effectiveness of such micropatterned bridges in their ability to partition cell population between reservoirs.

Cells were uniformly seeded on the micropatterns and allowed to partition over a 36 hr period (**Figure 3D;** Supplementary Data **Movie 2**). Partition patterns incorporating the spear-shaped patterns effectively guided on average 85% of the cells towards the top half of the partition pattern and on average 60% of the cells into the top (preferred) chamber. Similarly, partition patterns with teardrop patterns effectively guided on average 79% of the cells towards the top half of the pattern and on average 51% of the cells into the top chamber. On the other hand, control patterns partitioned equally on both sides with 51% of the cells towards the top half and only 27% of the cells into the top chamber. Fractions were employed to account for the proliferation of cells.

We can also gain some insight into the partition dynamics as we follow the time course of observed partitioning every 3 hours. During the initial 0-6 hr period, the cells must become mobile and become unilamellar and thus the fraction of cells remains unchanged. During the next 9-24 hr period, there is a rapid flux of cells through the micropatterned bridges towards the upper chamber. However, as the top chamber is clogged with cells, it becomes increasingly difficult to move upwards. Likewise, as the bottom chamber is emptied, the rate of entrance into the bridge section becomes the rate-limiting step. As a result, the partition fraction reaches a plateau, which is less than the bias dictated by the previous spear-shaped pattern analysis.

t = 0 hr t = 36 hr

(A) Spear-Shaped Partition Pattern

Total distance per bridge = 1502 µm

Average partition at 36 hr = 84.7%

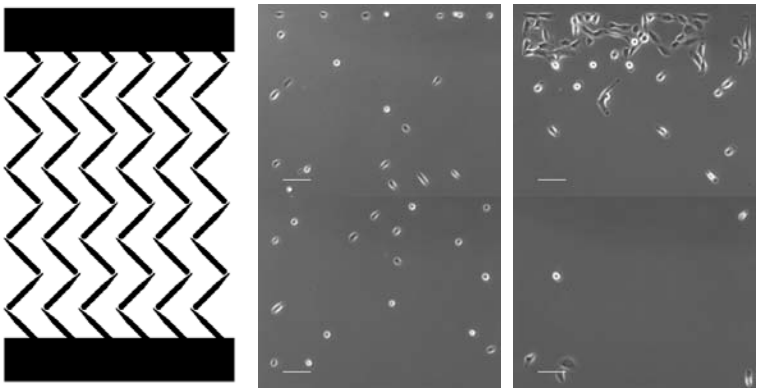

t = 0 hr t = 36 hr

(B) Teardrop Partition Pattern

Total distance per bridge = 2268 µm

Average partition at 36 hr = 79.4%

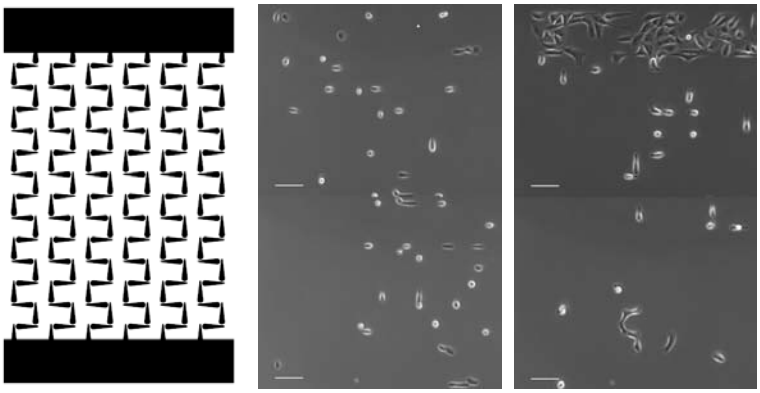

t = 0 hr t = 36 hr

(C) Control Pattern

Total distance per bridge = 1000 µm

Average partition at 36 hr = 51.1%

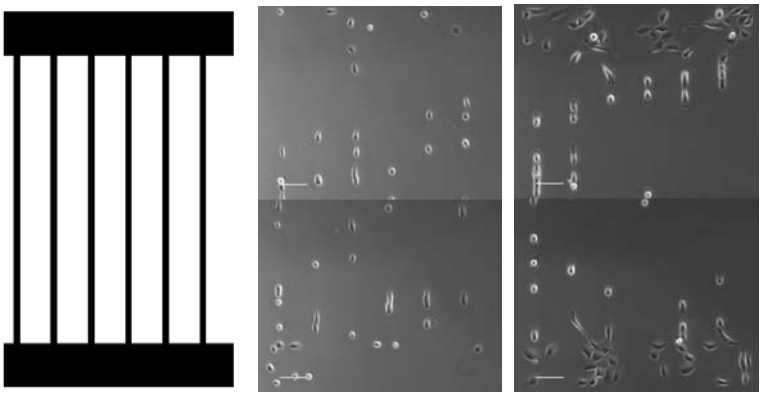

(D)

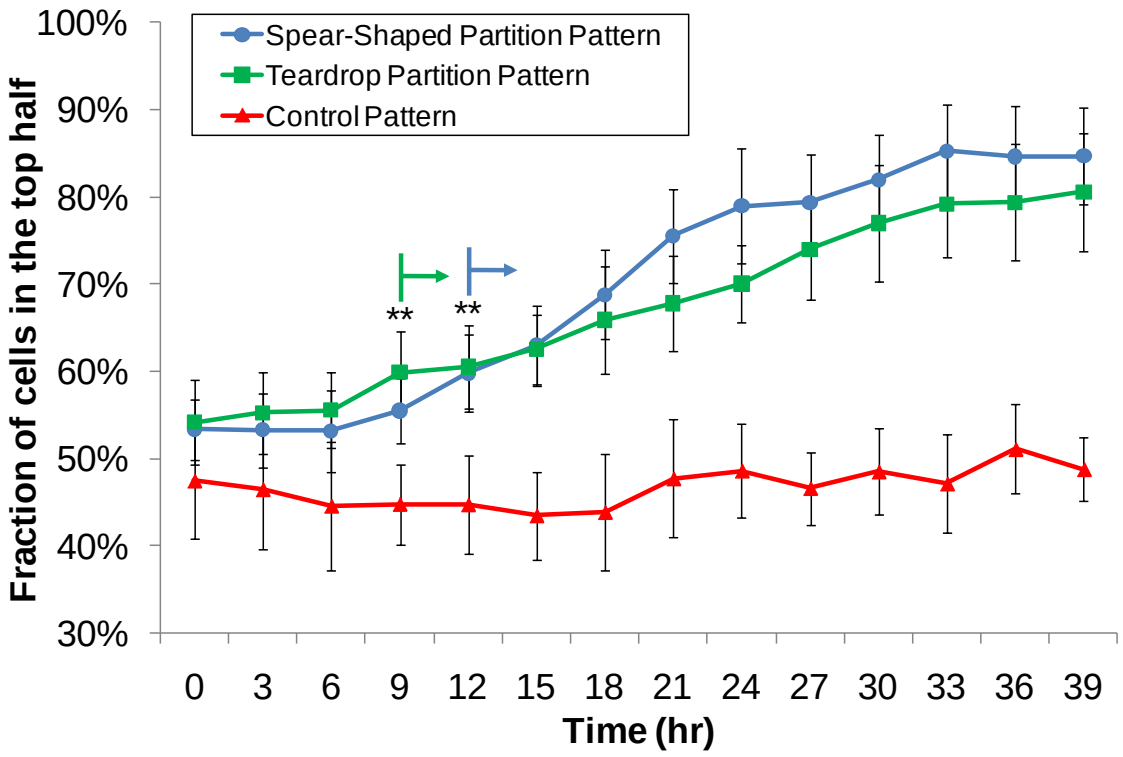

Figure 3. Schematic and effectiveness of partition patterns with spear-shaped and teardrop bridges. (A) The spear-shaped partition pattern and (B) the teardrop partition pattern guides the cells upwards, while (C) the control pattern does not [Scale bar = 100 μm]. (D) The fraction of cells in the top half of the pattern is plotted against time [**; $p<0.01$ (n=3, 8 patterns tested for each type)].

It is interesting to analyze the kinetics of partitioning in the multicellular context relative to the single-cell speeds measured in isolated spear-shaped patterns. The distance cells would have to travel through the bridge in the partitioning device is at most 1500 μm. Based on the observed single-cell net speed on spear-shaped patterns of 93

μm/hr, we can estimate that partitioning would occur in approximately 16 hr. However, it takes approximately 33 hr for partitioning to reach steady state after the initial 6 hr lag phase. This suggests that the rate of partitioning is retarded by phenomena not captured in the single-cell analysis. Such phenomena include cell-cell collisions, proliferation (as a side note, when a cell divides on a spear-shaped island, the two daughter cells initially migrate in opposite directions), island occupancy, etc. Consistent with the importance of multicellular phenomena in determining partitioning kinetics, we found that devices based on a teardrop bridge achieved the same extent of partitioning in a similar amount of time as a device based on spear patterns (**Figure 3D**). While the dynamics of multicellular behaviors are difficult to extrapolate solely from single cell migratory behavior, the effectiveness of the spear- and teardrop-based partitioning devices significantly surpass any previously reported micropattern-based partitioning.[11]

4. Conclusion

Geometrical constraints of micropatterns can govern cell motility. Some researchers have observed increased migration speed and persistence when cells are under width constraints.[3, 12] Also, we have previously shown that epithelial cells can exhibit directional movement on teardrop-based micropatterns.[5] This study focused on the potential to combine the enhanced speed and persistence on line patterns and the directional bias provided by the teardrop-based patterns for MCF-10A epithelial cells. The cell motility on this hybrid, spear-shaped pattern was found to exceed that on both of the original patterns and was quantitatively analyzed to understand the cause of the

enhancements. Furthermore, this hybrid pattern with enhanced motility was applied to partition designs to optimize the partition efficiencies of cell population, significantly surpasses that reported in previous works.[11] Thus, this study demonstrates the ability to effectively combine motifs of micropatterns to create hybrid patterns with synergistic outcomes and sheds light on the vast, underlying potentials in micropatterning technology.

5. Experimental Methods

5.1. Fabrication of micropatterned substrates

Microcontact printing with a polydimethylsiloxane (PDMS) stamp was used to pattern the adhesion ligand, as described previously.[5] Briefly, UV light is passed through a chrome mask containing the teardrop and spear-shaped patterns (Nanoelectronics Research Facility, UCLA) onto a layer of SU-8 negative photoresist to make a mold, onto which PDMS is cast to make the stamp. 16-Mercaptohexadecanoic acid (Sigma Aldrich) was printed with the stamp onto the gold-coated chambered coverslide (Fisher Thermo Scientific – NUNC). The unprinted area is passivated using PEG(6)-Thiol (Prochimia) so as to prevent protein adsorption and cell adhesion. The acid was then covalently bound to fibronectin to make cell adhesive patterns. Finally, BSA conjugated with Alexa Fluor 594 (Invitrogen) was doped to visualize the patterns (Chapter II Figure S4).

5.2. Cell culture

MCF-10A human epithelial cells were cultured in growth medium composed of Dulbecco's modified Eagle's medium/Ham's F-12 containing HEPES and L-glutamine (DMEM/F12, Invitrogen) supplemented with 5% horse serum (Invitrogen), 1% penicillin/streptomycin, 10µg/mL insulin (Sigma), 0.5µg/mL hydrocortizone (Sigma), 20ng/mL EGF (Peprotech) and 0.1µg/mL cholera toxin (Sigma) and maintained under humidified conditions at 37 ºC and 5% CO_2. Cells were passaged regularly by dissociating confluent monolayers with 0.05% trypsin-EDTA (Invitrogen) and suspending cells in DMEM/F12 supplemented with 20% horse serum and 1% penicillin/streptomycin. After two washes, cells were diluted 1:4 and plated in growth medium.

5.3. Timelapse microscopy

Cells were seeded in growth medium for 1h onto the micropatterned substrate. After washing to remove non-adherent cells, the culture was incubated with fresh growth medium for 1 hr and imaged at 10x magnification every 5min for 12hr (for single cell analysis) or every 3 hours for 36 hours (for multicellular analysis on partition patterns). Cells were maintained at 37ºC and 5% CO_2 in a heated chamber with temperature and CO_2 controller (Pecon) during time-lapse imaging. Images and movies were acquired using Axiovert 200M microscope (Carl Zeiss), and Axio Vision LE Rel. 4.7 (Carl Zeiss) was used for image analysis.

5.4. Data collection and analysis

For line patterns, the lamellipodial position was tracked using Axio Vision LE Rel. 4.7 and ImageJ software. Migration speed was obtained as the total distance traveled divided by the total time. The persistence length was based on switching the direction 180° and also on whether unilamellar morphology was broken or not (i.e., if a cell paused to spread and then eventually proceeded in the same direction, it was counted as a separate run).

For the speed and persistence calculation on classic teardrop and spear-shaped pattern analysis, a few assumptions were made. We assumed that for a cell to hop from one island to another island, it must travel 80 μm across the normal teardrop island and 180 μm across the spear-shaped island, and hop sideways across a 3 μm gap. If a cell starts or ends in the middle of an island, a method similar to line patterns were used to determine the auxiliary distance. Also, the residence times at each corner for each scenario (to hop or not to hop) were tracked separately; cells were considered as resident at a corner until their trailing edge was completely detached from that corner.

For the partition patterns, cells in the upper half of the pattern (one image) and the lower part of the pattern (another image) were counted for each pattern (cells that overlap between both images were considered as upper half). The data was expressed as percentages to account for the proliferation of cells. The bridge section was included because it is where a significant portion of the cells can reside (up to 70%) and also the most dynamic area of the pattern.

6. Acknowledgements

This research was funded by the NSF Center for Science and Engineering of Materials at Caltech. We also gratefully acknowledge the technical support and infrastructure provided by the Kavli Nanoscience Institute.

7. References

[1] D. M. Brunette, *Exp Cell Res* **1986**, *167*, 203.

[2] P. Clark, P. Connolly, A. S. Curtis, J. A. Dow, C. D. Wilkinson, *J Cell Sci* **1991**, *99 (Pt 1)*, 73.

[3] A. D. Doyle, F. W. Wang, K. Matsumoto, K. M. Yamada, *J Cell Biol* **2009**, *184*, 481.

[4] G. Kumar, C. C. Ho, C. C. Co, *Advanced Materials* **2007**, *19*, 1084.

[5] K. Kushiro, S. Chang, A. R. Asthagiri, *Advanced Materials* **2010**, n/a. doi: 10.1002/adma.201001619

[6] P. P. Provenzano, D. R. Inman, K. W. Eliceiri, S. M. Trier, P. J. Keely, *Biophys J* **2008**, *95*, 5374.

[7] E. Sahai, *Nat Rev Cancer* **2007**, *7*, 737.

[8] P. Clark, S. Britland, P. Connolly, *J Cell Sci* **1993**, *105 (Pt 1)*, 203.

[9] D. Gao, G. Kumar, C. Co, C. C. Ho, *Adv Exp Med Biol* **2008**, *614*, 199.

[10] B. Szabo, Z. Kornyei, J. Zach, D. Selmeczi, G. Csucs, A. Czirok, T. Vicsek, *Cell Motil Cytoskeleton* **2004**, *59*, 38.

[11] G. Mahmud, C. J. Campbell, K. J. M. Bishop, Y. A. Komarova, O. Chaga, S. Soh, S. Huda, K. Kandere-Grzybowska, B. A. Grzybowski, *Nature Physics* **2009**, *5*, 606.

[12] D. Irimia, M. Toner, *Integr Biol (Camb)* **2009**, *1*, 506.

Chapter IV: Scaling Micropattern Dimensions to Enable and Modulate Directed Cell Movement

1. Abstract

Micron-scale geometrical constraints shape cell morphology and affect cell motility. However, cell types differ in their response to geometric cues. Elucidating the underlying factors could instruct how to redesign micron-scale features to induce desired migratory properties in recalcitrant cell types. Here, we show that directional bias in cell movement on teardrop-based micropatterns is highly correlated to the establishment of a unilamellar morphology in fibroblasts, keratinocytes and mammary epithelial cells. Furthermore, narrowing the width of teardrop micropatterns enhances the establishment of a unilamellar morphology and increases the directional bias of movement of normal human epidermal keratinocytes (NHEK). These thin teardrops increase the bias of MCF-10A epithelial cells as well, but unexpectedly create a moderate bias on a previously unbiased configuration. These results give us insight into how cells can respond to different degrees of geometrical constraints (i.e., what cells interpret as tip as opposed to blunt) and how such constraints at the ends of the island dictate directional movement of cells on micropatterns. These findings underscore the importance of a unilamellar morphology in achieving directed cell migration on micropatterns and offer design strategies to promote directional bias in migration of different cell types for tissue engineering applications.

2. Introduction

Directional cell migration involves the establishment of front-rear (FR) polarity.[1, 2] The front is typically a broad lamella. Meanwhile, the narrow trailing end is more sensitive to myosin-generated contractile forces, facilitating the release of adhesions in the rear and net forward cell movement. The stability of FR polarity during cell migration is transient and helps in determining the persistence of the random walk in an isotropic microenvironment.

Micropatterns can influence the symmetry breaking process needed to establish and maintain FR polarity. For example, fibroblasts on extremely thin (1.5 μm) adhesive line patterns can break symmetry and assume a motile uniaxial morphology with a single lamella. [3] Furthermore, we have shown with MCF-10A epithelial cells that the spatial constraints imposed by micropatterned lines (20 μm width) forces single lamella that are narrower and more stable, leading to greater persistence in migration than observed on uniform substrates (Chapter III). Thus, the narrower, more stable lamella establishes and maintains a sharpened FR polarity and a distinct unilamellar morphology. Symmetry breaking is not unqiue to line patterns. Two cells occupying a circular island can break symmetry and start rotating in the same direction. Their yin-yang morphology is akin to the unilamellar morphology as well.[4]

Micropattern geometry can also give directional cues to cells. For example, Co and colleagues found that directional movement of 3T3 fibroblasts can be induced using teardrop-based micropatterns.[5] However, different cell lines can respond differently to

similar micropattern geometry. When a similar geometrical constraint was applied on MCF-10A epithelial cells, the movement bias was in the opposite direction.[6]

In this study, we sought to better understand how different cell lines interpret the underlying geometrical constraints and look for a universal predictor for directional cell movement. Perhaps, the establishment of the unilamellar morphology, which in itself represents directional orientation, is important in determining directional bias on these micropatterns. Furthermore, understanding the role of unilamellar morphology in directional cell movement on micropatterns may lead to more general strategies to modulate and enhance directional bias for all cell types.

3. Results

3.1. Cell types differ in the extent of directional bias on teardrop patterns

We previously showed that MCF-10A cells exhibit a high bias in movement on square migration tracks composed of teardrop-shaped micropatterns. [6] The cells traverse the track by hopping from one adhesive island to the next. A high bias is exhibited for hopping sideways from a tip to a blunt end (sT>B hop) when the teardrop patterns are arranged in Configuration A. No directional bias is observed in Configuration B, a track that lacks a junction for a sT>B hop (**Figure 1A**). These and other results demonstrated that the directional bias of MCF-10A cell movement stems from lamellipodial activity that extends preferentially sideways (not head-on) out of the tip ends of teardrop patterns. Enhancing lamellipodial stability by moderately reducing

the expression of Rac1 using siRNA interference enabled head-on lamellipodial extensions and flipped the directional bias of MCF-10A cell movement.

To test the generality of using teardrop micropatterns to direct cell migration, we examined the movement of other cell lines on the same teardrop-shaped micropatterns. Directional bias was quantified as the fraction of successful jumps in either the tip-to-blunt (T>B) or blunt-to-tip (B>T) direction. Normal human epidermal keratinocytes (NHEK) show a moderate bias on Configuration A with 66% of hops in the sT>B direction (**Figure 1B**, Supplementary Data **Movie 1**). While the preferred direction matches that of MCF-10A cells, the bias is quantitatively weaker in NHEKs. Similar to MCF-10A cells, NHEKs exhibit little to no bias on Configuration B (Supplementary Data **Movie 2**). Lastly, Rat1 fibroblasts show little to no bias on both configurations of teardrop patterns (**Figure 1C**, Supplementary Data **Movie 3)**. These results show that cell types differ significantly in the extent of directional bias, although where a bias is exhibited (moderate in NHEK and strong in 10A cells), the direction of cell movement consistently favors a sideway tip-to-blunt hop.

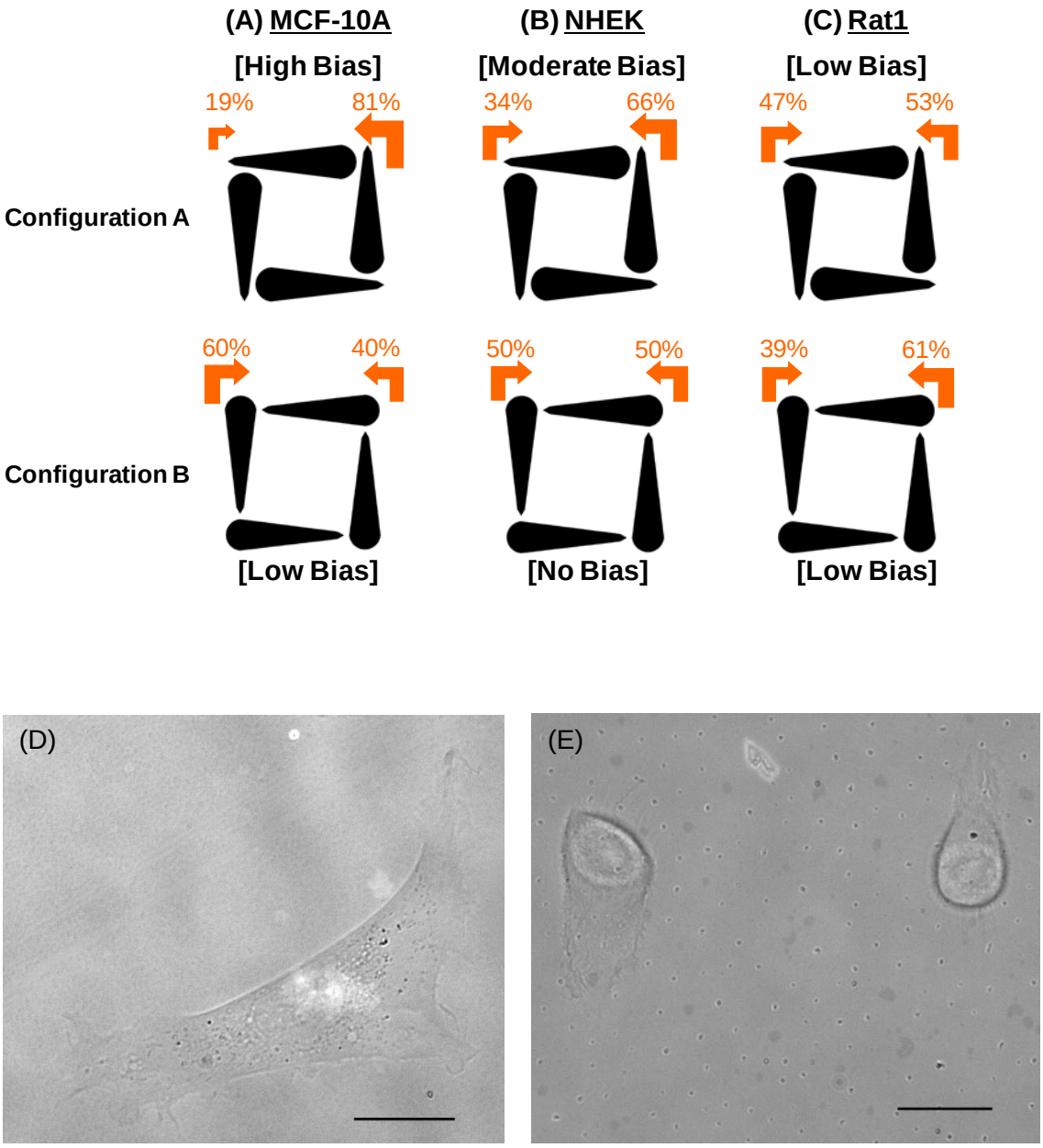

Figure 1. Motility biases for (A) MCF-10A epithelial cells, (B) NHEKs and (C) Rat1 fibroblasts on the original teardrop patterns. On Configuration A, MCF-10A epithelial cells showed high bias in the sideway tip to blunt direction, followed by moderate bias of NHEKs and no bias for Rat fibroblasts. (D) Rat1 fibroblasts on Pattern A do not establish any FR polarity, while (E) most of MCF-10A cells and some NHEKs establish a

strong FR polarity on Configuration A [Scale bar = 20μm]. On Configuration B, the cells showed relatively low to no bias.

3.2. Establishment of unilamellar morphology correlates with extent of directed cell movement on teardrop patterns

Qualitatively, we noticed that these cell types differ in the establishment of FR polarity. Rat1 fibroblasts and some of the NHEKs form lamellipodial fronts on two ends (i.e., no polarity), resulting in a tug-of-war between the two fronts and preventing directional movement (**Figure 1D**). On the other hand, almost all of the MCF-10A cells and many of the NHEKs establish a stable FR polarity with a single prominent lamella (**Figure 1E**),[6] closely resembling the unilamellar morphology observed in other studies.[3, 4] These observations suggested that the inability to establish or maintain unilamellar morphology may impair directional movement of NHEKs and the fibroblasts.

To probe more deeply the relationship between the unilamellar morphology and directed cell movement on teardrop patterns, we needed a technique to modulate the ability of cells to acquire the unilamellar morphology. Since unilamellar morphology was observed previously on extremely thin line patterns,[3] we hypothesized that the establishment of an unilamellar morphology may correlate with and be tuned by the width of the micropattern.

To test this idea, we plated the three cell types on micropatterned lines of different widths ranging from 5 - 20 μm and quantified the occurrence of unilamellar morphology.

We found that the line width affects the fraction of cells exhibiting the unilamellar morphology (**Table 1**). Almost all (92%+) of the MCF-10A cells become unilamellar within a 12-hour period on 20 micron lines; reducing the line width did not significantly enhance this saturated ability to attain a unilamellar morphology in 10A cells. Meanwhile, only 61% of the NHEKs become unilamellar on the 20 μm lines. This fraction increases significantly to 86% on thinner lines (5 and 10 μm). Almost none (<1%) of the Rat1 fibroblasts assume the unilamellar morphology on all line widths, consistent with the previous report that 3T3 fibroblasts exhibit a unilamellar morphology only on thin lines below 5 μm widths and predominantly on extremely thin lines of 1.5 μm width,[3] a feature size below the working range of our microcontact printing methodology.[7]

These quantitative measurements show that the ability of cells to acquire a unilamellar morphology is greatest for MCF-10A cells, followed by NHEKs and then Rat1 fibroblasts. This tendency to achieve unilamellar morphology correlates with the extent of biased movement on teardrop patterns, suggesting that establishment of such morphology may be critical to achieving directed movement. Furthermore, since narrowing line widths increases the occurrence of unilamellar morphology in NHEK cells, it presents an opportunity to test whether narrowing teardrop patterns may be a design strategy to induce or enhance directional bias in cell migration.

	Non-pattern	Line (5μm)	Line (10μm)	Line (20μm)
MCF-10A (epithelial cells)	N/A (~0%)	96%	96%	92%
NHEK (keratinocytes)	N/A (~0%)	86%	87%	61%
Rat1 (fibroblasts)	N/A (~0%)	1%	0%	0%

Table 1. Tendency to acquire unilamellar morphology for MCF-10A epithelial cells, NHEKs and Rat1 fibroblasts on line patterns of different widths. Fractions of cells that establish unilamellar morphology on the line patterns within the 12 hr-period immediately after seeding are shown. In general, greater constraint (thinner lines) seems to better promote the establishment of stable FR polarity resulting in unilamellar morphology.

3.3. Narrowing teardrop patterns enhances directional bias

To test the idea that narrowing the teardrop patterns may enhance directed cell movement on these micropatterns, we designed teardrop patterns with a maximum width of 10 μm at the blunt end and quantified cell migration on these thinner teardrop patterns (**Figure 2**). Other features of the square track, including the gap distance between teardrops and their relative positioning, were unchanged. The directional bias of NHEKs improved from 66% to 77%, a statistically significant ($p<0.05$) increase, on thin teardrops arranged in Configuration A (Supplementary Data **Movie 4**). Thus, increasing the occurrence of unilamellar morphology enhances directional bias of cell movement.

Although a similar increase was observed for Configuration B (50% to 60% in the head-on T>B direction), the cells jumped less frequently compared to Configuration A, and this change in directional bias was not statistically significant.

As a negative control, we tested the movement of Rat1 fibroblasts on the thinner teardrop patterns. Consistent with the fact that reducing line width to 10 μm had no effect on establishing unilamellar morphology in Rat1 fibroblasts, these cells exhibited no enhancement in directed cell movement on narrow teardrop patterns compared to the original teardrop patterns. Finally, MCF-10A cells, serving as positive control, maintained their high directional bias (81% to 86%, though not statistically significant) even on narrow teardrops in Configuration A, consistent with the fact that the fraction of unilamellar morphology remained near 95% on 10 and 20μm lines.

An unexpected observation, however, was the change in the movement of MCF-10A cells on thin teardrops in Configuration B, which offered additional insights into how cells interpret the rescaling of the teardrop pattern. Our quantitative measurements show that 10A cells on thin teardrops in Configuration B begin to mimic that of Configuration A (Supplementary Data **Movie 5**). Cells now actively hop sideways from the 10 μm blunt end onto the adjacent island's tip. This effect is also reflected in the increased frequency of hops on the narrow Configration B compared to the original Configuration B (data not shown). We conclude that at the 10 μm width, MCF-10A cells begin to respond to the blunt end as a tip, leading to the observed bias in sideways blunt-to-tip hops in the new Configuration B.

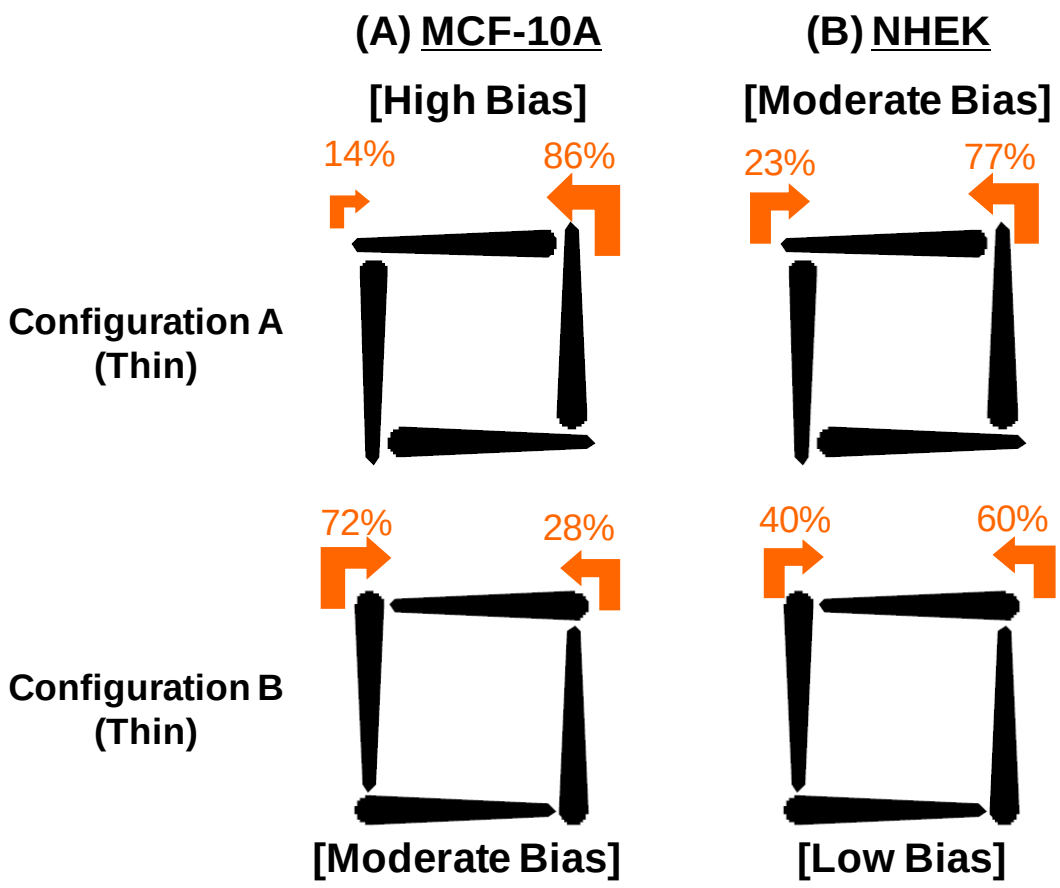

Figure 2. Motility biases for (A) MCF-10A epithelial cells and (B) NHEKs on thin teardrop patterns. On thin Configuration A, both MCF-10A epithelial cells and NHEKs showed significantly increased bias in the sideways tip to blunt direction compared to the original Configuration A. On thin Configuration B, the NHEKs showed relatively low bias, but the MCF-10A cells surprisingly showed a moderate bias in the sideways blunt to tip direction.

It is noteworthy that sideway extensions remain the preferred mode of hopping on the original and thinner teardrops. However, cells on the thin Configuration B exhibit

quantitatively less bias than on the original Configuration A. At least two factors may contribute to this quantitative difference in bias. First, the narrower blunt end (10 μm) is still wider than the tip end in Configuration A. Second, the degree of asymmetry in the narrower teardrop (the ratio of the widths of the blunt and tip end) is less than that presented by the original teardrop.

Taken together, these results demonstrate that the unilamellar morphology plays an important role in directed cell migration on teardrop patterns and show that narrowing teardrop patterns is a strategy to induce unilamellar morphology and enhance directed cell movement. In addition, although the unilamellar morphology is important, it is not sufficient. Approximately 95% of MCF-10A cells acquire unilamellar morphology on 10-20 μm lines but yet fail to exhibit biased movement on the original Configuration B. In addition to the acquisition of a unilamellar morphology, the geometrical constraints of the end from which cells hop are also critical. Adequate physical constraints (in the case of MCF-10A cells, an end constrained to ~10 micron width) must be imposed at a junction where a sideway hop can be executed to an adjacent island.

4. Future Directions

The new observation of increased migratory bias of MCF-10A cells on thin teardrops in Configuration B suggest that the geometric constraints at the ends of the teardrop and a properly positioned target island for a sideway hop may be more important than the asymmetry of the teardrop shape in dictating directional bias on micropatterns. To test this idea, we will parse out the contributions of asymmetry and geometrical

constraint by creating thin rectangles with widths of 5 and 10μm (**Figure 3**). In addition, extra thin teardrops with maximal width of 5μm will be tested on multiple cell lines to induce or enhance directed movement on micropatterns.

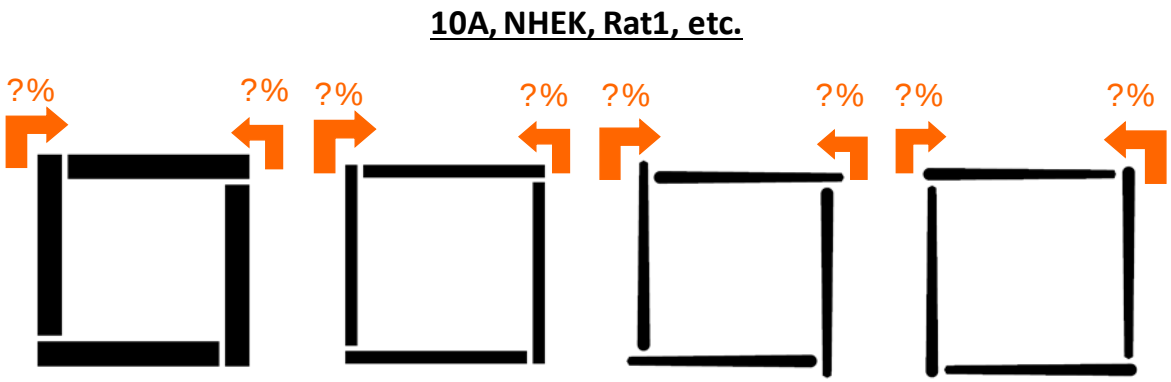

Figure 3. Schematics of thin rectangles and extra thin teardrop patterns to be tested with MCF-10A cells, NHEKs and other cell lines. The thin rectangles are 80μm in length and 10μm or 5μm in width with 3μm gaps. The extra thin teardrops are 80μm in length, 5μm wide at the blunt end and 3μm wide at tip end with 3μm gaps. The thin rectangles will reveal whether asymmetry is need for directional bias, and if so how large the impact is. Extra thin teardrops will be tested in an attempt to induce directional bias for other cell lines (such as fibroblasts), and also to look for similar trends in NHEKs as what we have observed for 10A cells.

5. Conclusion

Cell motility can be governed by the geometrical constraints imposed by the micropattern, but recent studies show that different cell types display different directional bias on similar patterns.[5, 6] In this study, we sought to understand why different cell

types may exhibit different directional bias on similar geometrical patterns, and utilize the findings to develop generalized strategies to control directed motility for different cell types. We compared the directed motility of three cell types on the teardrop-based micropatterns, and found a qualitative correlation between directional bias and their ability to assume unilamellar morphology. Further quantitative analysis using line patterns of different widths revealed that indeed the frequency of unilamellar cells correlates with the geometrical constraint of the lines. In an attempt to increase directional bias for some cell lines, we proceeded to scale-down the teardrop to the width corresponding to maximum frequency of unilamellar morphology and found that indeed the directional bias increases significantly. Furthermore, in addition to the necessity of unilamellar morphology in biased movement, we also found that the degree of geometrical constraints of the ends from which they jump also influences the directional bias. These findings begin to open venues to control the motility and directional bias of different cell types through scaling the dimensions of the patterns.

6. Experimental Methods

6.1. Fabrication of micropatterned substrates

Microcontact printing with a polydimethylsiloxane (PDMS) stamp was used to pattern fibronectin onto a gold-coated chambered coverslide (Labtek), as described previously.[6] Briefly, UV light is passed through a chrome mask containing the pattern (Nanoelectronics Research Facility, UCLA) onto a layer of SU-8 photoresist to make a mold, onto which PDMS is cast to make the final stamp. The stamp is then “inked” with

16-Mercaptohexadecanoic acid (Sigma Aldrich) to print the pattern onto a gold-coated coverslide. The unprinted area is passivated using PEG(6)-Thiol (Prochimia) to prevent non-specific binding of cells. After washing with PBS twice, EDC and Sulfo-NHS (Pierce) is added to the coverslide to activate the acid to crosslink covalently with the amine group of the subsequently added fibronectin (Sigma Aldrich) dissolved in PBS at 10μg/mL. Finally, BSA conjugated with Alexa Fluor 594 (Invitrogen) was doped into the fibronectin solution for the purpose of pattern visualization.

6.2. Cell culture

MCF-10A human epithelial cells were cultured in growth medium composed of Dulbecco's modified Eagle's medium/Ham's F-12 containing HEPES and L-glutamine (DMEM/F12, Invitrogen) supplemented with 5% horse serum (Invitrogen), 1% penicillin/streptomycin, 10 μg/mL insulin (Sigma), 0.5 μg/mL hydrocortizone (Sigma), 20ng/mL EGF (Peprotech) and 0.1 μg/mL cholera toxin (Sigma) and maintained under humidified conditions at 37ºC and 5% CO_2. Cells were passaged regularly by dissociating confluent monolayers with 0.05% trypsin-EDTA (Invitrogen) and suspending cells in DMEM/F12 supplemented with 20% horse serum and 1% penicillin/streptomycin. After two washes, cells were diluted 1:4 and plated in growth medium.

Normal human epidermal keratinocytes (NHEKs) were cultured in keratinocyte growth medium-2 (KGM-2, Lonza) and maintained under conditions at 37ºC and 5% CO_2. Cells were passaged regularly according to instructions provided by Lonza. Briefly,

confluent monolayers were dissociated with trypsin/EDTA (Lonza) and cells suspended in trypsin neutralizing solution (TNS, Lonza). After two washes with HEPES Buffered Saline (Lonza), cells were diluted 1:4 and plated in KGM-2.

Rat1 fibroblasts were cultured in growth medium composed of Dulbecco's modified Eagle's medium (DMEM, Invitrogen) supplemented with 10% fetal bovine serum (FBS, Invitrogen) and 1% penicillin/streptomycin and maintained under humidified conditions at 37ºC and 5% CO_2. Cells were passaged regularly by dissociating confluent monolayers with 0.05% trypsin-EDTA (Invitrogen) and suspending cells in growth medium. After two washes, cells were diluted 1:10~1:12 and plated in growth medium.

6.3. Timelapse microscopy

Cells were seeded in growth medium for 1 hr onto the micropatterned substrate. After washing to remove non-adherent cells, the culture was incubated with fresh growth medium for 1 hr and imaged at 10x magnification every 5 min for 12 hr. Cells were maintained at 37ºC and 5% CO_2 in a heated chamber with temperature and CO_2 controller (Pecon) during time-lapse imaging. Images and movies were acquired using Axiovert 200M microscope (Carl Zeiss), and Axio Vision LE Rel. 4.7 (Carl Zeiss) was used for image analysis.

6.4. Cell motility quantitation and analysis

For line patterns, the lamellipodial position was tracked using Axio Vision LE Rel. 4.7 and ImageJ software. The tendency to establish FR polarity was determined as the fraction of cells that assume FR polarity at one point or another during the course of a 12-hr experiment. Also, migration speed was obtained as the total distance traveled divided by the total time, and the persistence length was based on switching the direction 180° (not based on whether FR polarity was broken or not).

The directional biases on teardrop-based patterns were obtained as described previously,[6] which are fractions of the complete successful jumps in each direction of the pattern. Degree of bias was arbitrarily assigned as “no bias” (50%), “low bias” (51~65%), “moderate bias” (66%~80%) and “high bias” (81%~).

7. Acknowledgements

We thank the members of the Asthagiri group for helpful discussions. This research was funded by the NSF Center for Science and Engineering of Materials at Caltech. We also gratefully acknowledge the technical support and infrastructure provided by the Kavli Nanoscience Institute.

References

[1] D. A. Lauffenburger, A. F. Horwitz, *Cell* **1996**, *84*, 359.

[2] A. J. Ridley, M. A. Schwartz, K. Burridge, R. A. Firtel, M. H. Ginsberg, G. Borisy, J. T. Parsons, A. R. Horwitz, *Science* **2003**, *302*, 1704.

[3] A. D. Doyle, F. W. Wang, K. Matsumoto, K. M. Yamada, *J Cell Biol* **2009**, *184*, 481.

[4] S. Huang, C. P. Brangwynne, K. K. Parker, D. E. Ingber, *Cell Motil Cytoskeleton* **2005**, *61*, 201.

[5] G. Kumar, C. C. Ho, C. C. Co, *Advanced Materials* **2007**, *19*, 1084.

[6] K. Kushiro, S. Chang, A. R. Asthagiri, *Advanced Materials* **2010**, n/a. doi: 10.1002/adma.201001619

[7] G. M. Whitesides, E. Ostuni, S. Takayama, X. Jiang, D. E. Ingber, *Annu Rev Biomed Eng* **2001**, *3*, 335.